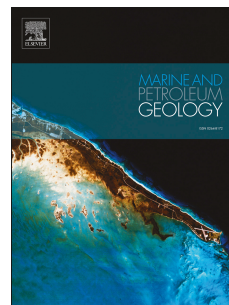


Accepted Manuscript

Interpretation of the Penobscot 3D Seismic Volume Using Constrained Sparse Spike Inversion, Sable sub-Basin, Offshore Nova Scotia

Taylor J. Campbell, F.W. (Bill) Richards, Ricardo L. Silva, Grant Wach, Leslie Eliuk



PII: S0264-8172(15)30061-1

DOI: [10.1016/j.marpetgeo.2015.08.009](https://doi.org/10.1016/j.marpetgeo.2015.08.009)

Reference: JMPG 2317

To appear in: *Marine and Petroleum Geology*

Received Date: 17 April 2015

Revised Date: 31 May 2015

Accepted Date: 6 August 2015

Please cite this article as: Campbell, T.J., Richards, F.W.(B.), Silva, R.L., Wach, G., Eliuk, L., Interpretation of the Penobscot 3D Seismic Volume Using Constrained Sparse Spike Inversion, Sable sub-Basin, Offshore Nova Scotia, *Marine and Petroleum Geology* (2015), doi: 10.1016/j.marpetgeo.2015.08.009.

This is a PDF file of an unedited manuscript that has been accepted for publication. As a service to our customers we are providing this early version of the manuscript. The manuscript will undergo copyediting, typesetting, and review of the resulting proof before it is published in its final form. Please note that during the production process errors may be discovered which could affect the content, and all legal disclaimers that apply to the journal pertain.

**Interpretation of the Penobscot 3D Seismic Volume Using Constrained Sparse
Spike Inversion, Sable sub-Basin, Offshore Nova Scotia**

Taylor J. Campbell^{a*}, F.W. (Bill) Richards^a, Ricardo L. Silva^a, Grant Wach^a, Leslie Eliuk^a.

*Basin and Reservoir Lab, Department of Earth Sciences, Dalhousie University, Halifax, Nova Scotia, B3H 4J1 Canada. taylor.campbell@dal.ca, billrichards888@hotmail.com; ricardo.silva@dal.ca; grant.wach@dal.ca; leslie.eliu@dal.ca.

*Corresponding author:

Taylor Campbell

Tel.: +1 902 494 8019

E-mail: taylor.campbell@dal.ca

Abstract

In this study we investigate the utility of constrained sparse spike inversion (CSSI) applied to a small (87 km^2), public domain, 3D seismic volume at Penobscot in the Sable sub-Basin, offshore Nova Scotia. The objective is to establish the effectiveness of this technique at Sable, in mapping absolute acoustic impedance that can be directly and quantitatively related to lithology. The intent is to subsequently apply the workflow to large 3D seismic volumes sub-regionally, with the goal of identifying and mapping, source, seal, reservoir, and overpressured intervals either not known, or partially known, from well control. *Absolute* acoustic impedance is an incremental parameter that is not explicit in the reflection amplitude cube and is the primary driver for undertaking this inversion. It has quantitative advantages over *relative* acoustic impedance that can be derived using ‘fast-track’ inversion techniques. CSSI at Penobscot has been completed and provides a valid geological model in the upper Jurassic to lower Cenozoic interval that is constrained by wireline logs at two well penetrations (one of which has 12m net pay). This acoustic impedance volume facilitates interpretation of: (1) low impedance Cretaceous reservoir sandstones, in both complex confined channel systems and extensive unconstrained marginal marine systems; (2) polygonal fault systems (PFS) in a high impedance, late Cretaceous, chalk; (3) interfingering of low impedance shales and high impedance carbonates at the margin of the Jurassic Abenaki Carbonate Bank.

Three other inversion studies have been reported at Penobscot: Ahmad, 2013; Sayers 2013; Qayyum, 2014. Relative acoustic impedance is derived in each study, using ‘recursive’, ‘spectral’ and ‘coloured’ inversion algorithms respectively. None of these studies documented the PFS and Cretaceous channel systems described here and there are significant interpretation differences in the Jurassic section, which is only partly penetrated by wells at Penobscot.

Based on this work at Penobscot, CSSI is the optimum technique for progressively building large sub-regional scale inversions at Sable where we need to balance work-effort, signal-to-noise ratio (spectral inversion results are very broadband but appear very noisy), reliable quantitative mapping of absolute acoustic impedance, and the identification of stratigraphic features on horizon-slices (for which ‘fast track’ inversions are also be suitable).

Keywords: acoustic impedance; seismic inversion; constrained sparse spike inversion; hydrocarbons; polygonal fault systems; Penobscot 3D dataset; Scotian Basin; Canada.

1. Introduction

Since 1959, when exploration licences were awarded near Sable Island, over 200 wells have been drilled on the Scotian margin (Figure 1). Approximately 400,000 km of 2D seismic data and 29,000 square kilometres of 3D seismic data have been acquired (Catuneanu, 2006). On this, passive margin of the Atlantic Ocean, there have been twenty-three significant hydrocarbon discoveries since 1967. Eight discoveries were commercial. Two commercial projects are currently producing hydrocarbons: gas from the Cretaceous and Jurassic clastic reservoirs in the five fields of the Sable Offshore Energy Project (since 1999); and gas from Jurassic carbonate reservoirs in the Deep Panuke Project (since 2013). The Cohasset-Panuke Project produced 44.5 MBO between 1992 and 1999 from Cretaceous clastic reservoirs (of similar age to thin, <5 m, hydrocarbon bearing zones at Penobscot).

The hydrocarbon system at Sable is gas prone, sourced from marginal marine shales that contain lean, but pervasive, terrestrially derived Type III organic matter (Wade and MacLean, 1990). With two exceptions, commercial hydrocarbons at Sable are trapped in Cretaceous and late Jurassic, marginal-marine, clastic reservoirs in rollover anticlines associated with down-to-basin listric faults, some of which have salt movement in the footwall. Multiple non-commercial accumulations are similarly trapped. Where these traps are fault dependent (or become fault dependent at the limit of independent, four-way dip closure) hydrocarbon column heights are controlled by cross-fault reservoir connections, which allow upward leak of hydrocarbons to levels above trap closure (Richards, 2008). At Deep Panuke, hydrocarbons are in Jurassic carbonate reservoirs, in a complex structural, stratigraphic, diagenetic trap (Wierzbicki, 2005 & 2010; Weissenberger 2006; Eliuk, 2010). At Cohasset-Panuke clastic reservoirs are draped over

the carbonate bank margin. At Penobscot the proven hydrocarbon trap is a four-way dip closure in the hanging wall of a listric fault (that occurs above the carbonate bank margin).

The seismic, well and production data based on the Scotian margin has been systematically archived and studied by the Canada Nova Scotia Offshore Petroleum Board (CNSOPB) and the Geological Survey of Canada (GSC). It is almost entirely in the public domain and is available through the CNSOPB's Data Management Centre and the GSC's online 'BASIN' database. Seismic data are available in 'hardcopy' format, which includes digital images but not SEGY files. One exception is the 87 km² Penobscot 3D seismic cube (location, Figure 1), which is owned by the province and is available to the public through the CNSOPB at no charge (downloadable from the Open Seismic Repository, see supplementary data section).

The Penobscot 3D seismic cube is of very good quality in the Cretaceous and Cenozoic section and is structurally simple. The cube provides an excellent opportunity (outside energy companies or government agencies) to interpret, manipulate and publish digital seismic data from the Sable sub-Basin in a workstation environment where modern techniques such as attribute analysis and seismic inversion can be implemented. Interpretations in this study were undertaken using the Petrel platform (courtesy of Schlumberger) and inversion was undertaken using InverTracePlusTM (courtesy of Jason Geophysical).

In this paper we present interpretation of the Penobscot 3D cube comparing conventional 'seismic facies' and attribute interpretations from a reflection amplitude cube to lithological interpretations from an acoustic impedance cube. There are sufficient acoustic impedance contrasts between lithologies at Penobscot to yield reflection patterns and reflection amplitudes that can be interpreted stratigraphically in both section-view and map-view (particularly when horizon-to-horizon interval attributes are examined, or horizon-slices are inspected after the cube

has been flattened on structural markers). Transformation to acoustic impedance enables direct interpretation of lithologies, particularly high impedance limestones and tight sandstones, low impedance reservoir quality sandstones and deep-water distal shales.

Many approaches to amplitude inversion (as opposed to velocity inversion) have been developed and these can be split broadly into acoustic and elastic inversions. Acoustic impedance inversion is explicitly stated as ‘transformation of post-stack seismic reflection data to P-impedance layer data’ in the InverTracePlus™ training manual.

Acoustic impedance inversion is conceptually a reversal of the forward convolutional model commonly used to generate synthetic seismograms from well log data. In forward modeling, reflection coefficients calculated from acoustic impedance (via sonic & density well logs) are convolved with a wavelet estimated from the seismic data to produce a synthetic seismic trace. In practice, inversion is often actually accomplished by repeating the forward modeling process iteratively many times, until a ‘best fit’ of the forward model to real seismic data is achieved at each seismic trace. The initial impedance model at each trace (including a low frequency trend below seismic frequencies) is first propagated throughout the seismic data set from well ties, using key interpreted seismic horizons as control.

There is an assumption of normal incidence, zero-offset ray paths in acoustic inversion and so the mode conversions that occur between P-waves and S-waves when ray paths are oblique to interfaces are not taken into account – and these are fundamental to fluid effects on seismic data. Acoustic inversion therefore has limitations in discriminating lithological and fluid effects, which are addressed more rigorously by elastic inversion techniques. At Penobscot the two wells within the 3D survey tested low relief two-way-time closures and are predominantly wet (~12 m net pay in ~1000 m of wet, net porous sand in the two wells), and so this should not

be a limitation in this study. In general, the Cretaceous Missisauga Formation and the Jurassic Micmac Formation reservoirs in the Sable sub-Basin are consolidated sandstones with possibly subtle amplitude effects where gas filled. In the shallow Logan Canyon reservoirs above the West Sable salt dome, conventional ‘bright spots’ with flat reflection terminations have been observed (Richards, 2008).

There are various approaches to acoustic impedance inversion in the oil industry. InverTracePlus™ is a Constrained Sparse Spike Inversion (CSSI), which is a type of iterative, model-based inversion known as Generalized Linear Inversion (Cooke and Cant, 2010). Iterative, model based, inversions are computationally intensive but efficiencies can be achieved by optimizing the number of reflection coefficients in each modeled trace and by optimizing the number of iterations required to converge on a satisfactory solution at each trace, which may be non-unique. For commercial reasons the precise procedures are often not described in detail.

In addition to enabling quantitative predictions of reservoir properties (Ma, 2000), the inversion process is purported to attenuate wavelet effects, reduce side-lobes and tuning effects, and possibly extend resolution beyond the seismic band (e.g. Barclay et al., 2008; Fichtner, 2011; Zhou, 2014).

There are three inversion studies at Penobscot publically available, each using different inversion algorithms. Ahmad (2013) reports on a ‘recursive inversion’ of the Jurassic section at Penobscot and provides a single vertical section with a tie to the Penobscot B-41 well (which just ‘tags’ the Jurassic carbonate), a single impedance slice, and a lithology-porosity cross plot. Recursive inversion became common in the late 1970s and employs a simple algorithm based on the assumption that each seismic sample represents a reflection coefficient (Lindseth, 1979;

Pendrel, 2006; Lines and Alam, 2013). Given an assumed acoustic impedance in the top layer, the acoustic impedance of all subsequent layers can then be calculated.

Sayers, 2013 performed a ‘spectral inversion’ (Puryear and Castagna, 2008) on a 10 km² subset of the 87 km² Penobscot cube. This technique incorporates thin bed information obtained by short-window Fourier analysis of the seismic data to improve vertical resolution. Significant success is reported: ‘vertical resolution in this area was improved from 61 m to 21 m,’ and, ‘frequency content of the inversion volume increased, with the dominant frequency improving from 29 Hz to 83 Hz,’ however the data appear very noisy. Sayers interprets both the outboard and inboard margins of the Abenaki Carbonate Bank within the Penobscot survey, and then focuses on the thickness and structure of sandstones in the Middle Missisauga Formation and the identification of small throw faults. These faults are then inferred to constitute a potential leak mechanism.

Qayyum (2014) addresses application of sequence stratigraphic principles to the mixed siliciclastic-carbonate setting associated with the Abenaki Carbonate Bank. A ‘fast-track’ inversion algorithm, ‘coloured inversion’, was applied to the Penobscot cube. Horizon slices and vertical displays of the Jurassic section from this inversion form part of a substantial sub-regional sequence stratigraphic study. Coloured inversion is described as a ‘fast track’ technique by the developers (Lancaster and Whitcombe, 2000), aimed at non-specialists that ‘performs significantly better than traditional fast track routes, such as recursive inversion’. The technique assumes zero phase data and uses a single operator to derive acoustic impedance.

The objective of this study is to apply a rigorous, industry-standard inversion technique at Penobscot, report on the results, and where they are new, useful and positive and to recommend further application to much larger data sets in the basin. The intent is not to compare the merits or utility of different inversion algorithms (see Cooke and Cant, 2010, for an excellent

discussion) or the value of inversion in principle. On this topic Pendrel (2001) begins with a question worth repeating, ‘Is it just coloured seismic with a 90 degree phase rotation or a unique window into the reservoir?’. At Penobscot we see incremental value in the inversion simply because it enables the interpreter to deal with a parameter directly linked to lithology that enables high confidence interpretation beyond well control. We focus carefully on the actual absolute acoustic impedance values in the well logs and subsequent inversion.

It is difficult to compare the recursive, coloured and constrained sparse spike inversions at Penobscot without having the relevant cubes loaded to a workstation. It is likely that the ‘fast track’ techniques provide similarly useful rendition of stratigraphic geometries but are less accurate in quantitative acoustic impedance prediction. The spectral inversion data set is a small subset of the Penobscot volume and is reported to have spectacularly wider bandwidth (far out into the noise on the other data sets) and higher resolution, which is apparent on published displays but appears very noisy. Assessing this inversion in detail relative to well control and in horizon-slice view would also require loading to a workstation.

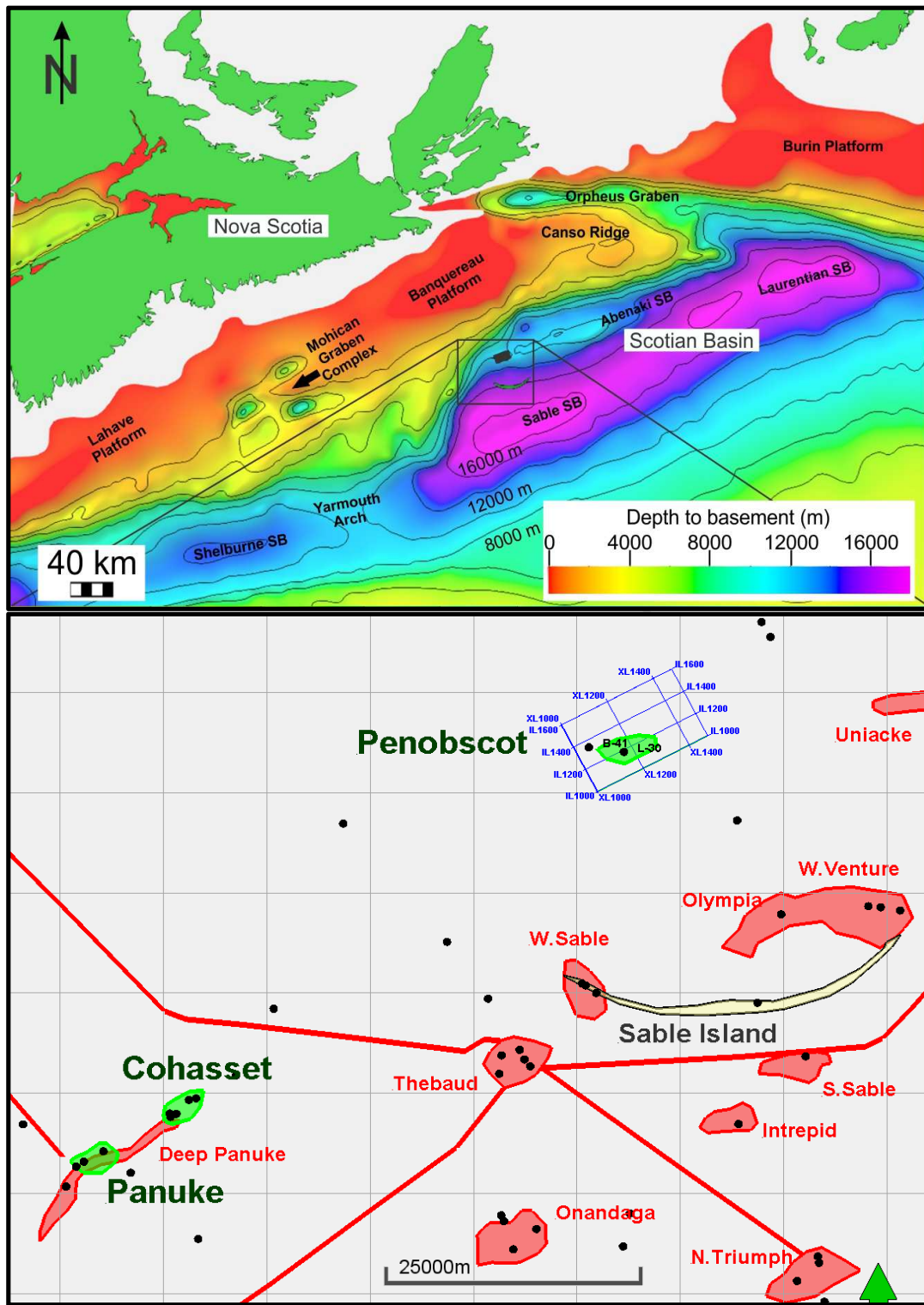


Figure 1: Scotian shelf sub-basins and location of the Penobscot 3D, wells and nearby fields and pipelines.

2. Geological Background

The Scotian Basin, offshore Nova Scotia, extends over approximately 300,000 km² (Hansen et al, 2004). It is subdivided into four sub-basins; Laurentian, Abenaki, Sable and Shelburne and is flanked by three plateaux: Burin, Banquereau and LaHave (e.g. Williams and Grant 1998).

During the break-up of Pangaea, the North American plate began to separate from the African plate. The initial rifting phase in the Middle Triassic created several interconnected rift basins, including the Scotian Basin. Initial sedimentation, infilling topographic lows, comprised volcanics rocks associated with rifting and fluvial red bed sediments in the lower part of the Eurydice Formation (e.g. Wade and MacLean, 1990; Wade et al., 1995). A generalized stratigraphic chart is presented as Figure 2.

Throughout the Middle Triassic and Late Triassic the North American and African plates shifted northwards, positioning the Nova Scotia region in a sub-equatorial area that had an arid climate (e.g. Olsen et al., 2000, 2003). Rifting and deposition continued throughout the late Triassic when topographic barriers were breached and marine waters from the eastern Tethys paleo-ocean flooded interconnected syn-rift basins. Terrestrial, and restricted shallow marine conditions, arid climate, and varying subsidence resulted in deposition of mixed clastics, minor carbonates and minor evaporites in the upper part of the Eurydice Formation, coeval with deposition of massive salt and anhydrite beds of the Argo Formation (Wade and MacLean, 1990; Wade et al., 1995) (Figure 2).

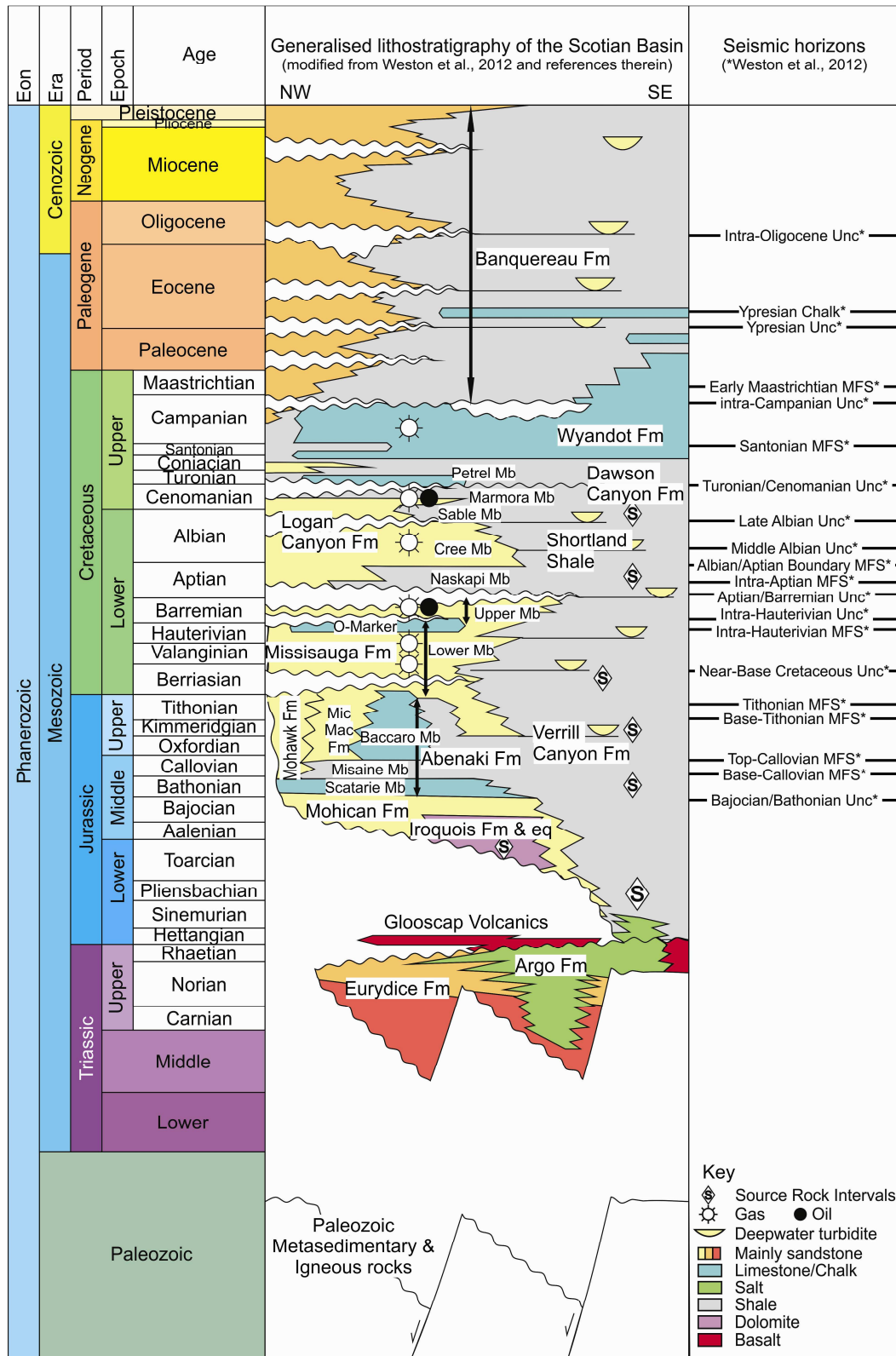


Figure 2: Generalized stratigraphic chart of the Scotian Margin (modified from Wade and MacLean, 1990).

In the Late Triassic–Early Jurassic, tectonism continued, culminating in the formation of a break-up unconformity, when North America and Africa separated completely, forming the proto-Atlantic Ocean (e.g. Wade and MacLean, 1990; Shimeld, 2004; Labails et al., 2010; Sibuet et al., 2012). After break-up, the Scotian Basin was flooded by a shallow marine sea, within which carbonates and clastics of the Iroquois Formation were deposited. This was followed by deposition of coarse clastic fluvial sediments: the Mohican Formation (Wade and MacLean, 1990; McIver, 1972).

During the Middle–Late Jurassic (Bathonian–Tithonian, see Weston et al., 2012) the Scotian Basin attains great depositional complexity. This interval includes the coeval Abenaki, Mohawk, Micmac, and Verrill Canyon Formations and the Lower Member of the Missisauga Formation (Figure 2).

The Abenaki Formation, located in the southwestern part of the basin, was deposited during the Jurassic in a period of basin subsidence due to sea floor spreading. It comprises a broad carbonate platform developed along the basin hinge zone, which inter-fingers with finer grained sediments deposited in deeper water (e.g. Eliuk, 1978; Kidston et al., 2005). Broadly, the Abenaki Formation is made up of two carbonate members (the Scatarie and Baccaro) separated by a sub-regional shale member (the Misaine) near the base. In more detail, Weissenberger et al (2000) recognise six carbonate cycles. The Scatarie is designated as ‘Abenaki I’ the Misaine and Lower Baccaro as ‘Abenaki II’, with four subsequent Baccaro cycles above, ‘Abenaki III-VI’.

The Mohawk Formation and MicMac Formation are clastic formations, coeval with the Abenaki Carbonate Bank. The Mohawk Formation is inboard of the bank, the MicMac both inboard and outboard. The Verrill Canyon Formation is a distal clastic formation, coeval with, and outboard of, the Abenaki Carbonate Bank. It interfingers with both the Abenaki and the

MicMac Formations. The Verrill Canyon Formation also interfingers with the overlying Cretaceous Missisauga Formation.

The Mohawk Formation comprises feldspathic sandstones and siltstones with interbedded shale and limestones (e.g. McIver, 1972; Given, 1977). The MicMac Formation comprises fluvio-deltaic sands interbedded with tongues of pro-delta shales (Verrill Canyon Formation) and was deposited during the Late Jurassic, marking the initial phase of uplift of the hinterland and progradation of the Sable Delta (e.g. McIver, 1972; Jansa and Wade, 1975; Beicip-Franlab, 2011) (Figure 2). The Lower Member of the Missisauga Formation consists of sandstone and minor thin limestones within a section of grey marine shales (e.g. Beicip-Franlab, 2011).

Deposition of fluvio-deltaic sediments continued into the Early Cretaceous (Berriasian/Valanginian–Barremian) forming the Middle and Upper members of the Missisauga Formation (e.g. Wade and MacLean, 1990; Pe-Piper and MacKay, 2006). The ‘O’ Marker (a diachronous, carbonate, seismic marker on the shelf) separates the Lower and Middle Missisauga Members from the Upper Missisauga member (Jansa et al., 1990; Beicip-Franlab 2011). The Upper Missisauga Member is limited to the north by an erosional edge on the LaHave Platform (e.g. Beicip-Franlab, 2011).

Deltaic sedimentation continued above the Missisauga Formation into the Aptian-Cenomanian, Logan Canyon Formation, but slow transgression and progressive deepening resulted in an overall upwards decrease in sandstone bed thickness, diminishing net-to-gross ratios, and reduced grain size, (Jansa and Wade, 1975). The Logan Canyon Formation is subdivided into four members, two of which are shale dominated: the Naskapi and Sable

Members. In this study lower coastal plain / shallow marine channel complexes observed seismically in the Cree and Marmora Members of the Logan Canyon Formation are described.

Above the Logan Canyon Formation, transgression continued with deposition of the Dawson Canyon Formation marine shale, and culminated in the Campanian-Maastrichtian with deposition of the Wyandot Formation Chalk (Jansa and Wade, 1975). A thin chalk, the Petrel Member of the Dawson Canyon Formation, is an important seismic marker on the Scotia Shelf. Polygonal fracturing, observed seismically here in the Wyandot Formation, is common in chalks on the Atlantic margin of Canada and in the North Sea. A number of mechanisms for such polygonal fault systems (PFSs) have been proposed, including shallow overpressure development, abnormal gravitational loading, differential compaction, diagenesis and syneresis (Cartwright, 2014; Hansen, 2004; Smith, 2010).

Cenozoic sediments above the Wyandot Formation constitute the Banquereau Formation (McIver, 1972) deposited as a progradational system of mudstones, subordinate marls and sandstones in relatively deep water, interrupted by several hiatuses, or, sub-aqueous unconformities (e.g. McIver, 1972; Jansa and Wade, 1975; Hansen et al., 2004; Deptuck and Campbell, 2012). Regression and increased coarse clastic deposition in the Late Oligocene culminates in glacial and peri-glacial conditions in the late Pliocene (Jansa and Wade, 1975).

The Banquereau Formation is overlain by the Quaternary Laurentian Formation, which comprises glacial drift and stratified pro-glacial material (Jansa and Wade, 1975).

3. Penobscot

The Penobscot area is currently unlicensed. No bids were received in the 2013 CNSOPB Call for Bids (see <http://callforbids.cnsopb.ns.ca/2013/01/>). The CNSOPB has provided

substantial technical analysis of the Penobscot area online (e.g.: http://callforbids.cnsopb.ns.ca/2013/01/sites/default/files/inline-pdf/table_a_ns13-1_hydrocarbon_wells_reservoir_properties.pdf).

3.1. Penobscot L-30 and Penobscot B-41 Wells

The Penobscot L-30 well was drilled by PetroCanada-Shell in 1976 and recovered hydrocarbons from four Middle Missisauga sandstones. The well tested the eastern flank of a west-east trending structural high (Figure 3, Top Middle Missisauga time structure map) in the hangingwall of a down-to-basin fault (Figures 4 and 5, reflection amplitude and acoustic impedance dip lines through the well.). The structural high tested by L-30 has two structural culminations, one up-dip immediately to the west of L-30, and a second further west, separated by a time saddle, and tested by the Shell-PetroCanada B-41 well in 1977. The B-41 well was entirely wet apart from 1m of oil pay described in core. Above Top Middle Missisauga level all time structure maps derived from the 3D survey show that the L-30 well is outside structural closure and the wet well results in these intervals are consistent with this. Only the Top Middle Missisauga time structure map is included here. At B-41, time structure maps at Top Naskapi, Top Upper Missisauga, Top Middle Missisauga and Top Lower Missisauga show 10-15 msecs of independent closure which is not consistent with the well result, either because hydrocarbons did not enter the trap, which is unlikely at Sable where all trap space appears to be filled – wet, and valid traps have not been reported, or because the mapped time closure is not a closure in depth due to velocity variations in the overburden. This is the more likely explanation. Time to depth error of 25 m in 2500 m (1%) would not be unusual. Near seabed channels are observed above the B-41 structure and time ‘sags’ beneath shallow channels are common at Sable (see section

4.2). Another possibility is that thin, intraformational seals, were breached by erosional channels or minor faults (as per Sayers, 2013) but it is not obvious why this would happen in one culmination and not the other. The aquifer system is normally pressured so top seal failure by mechanical or capillary leak is very unlikely.

At Top Middle Missisauga level the L-30 well is at the limit of an independent time closure and, consistent with this, the well results indicate that it is at the very limit of an effective hydrocarbon trap. Seven sandstones (designated Sands 1-7) are interpreted by the CNSOPB to have encountered both hydrocarbons and water, based on repeat formation tests (RFTs) and logs in Sands 1-4, and log interpretation in Sands 5, 6 and 7 (CNSOPB, 2013). These Middle Missisauga sandstones are annotated on wells logs in Figure 6 and again in Figure 7 in more detail where RFT results are added. Three oil, four condensate, four minor gas, and twelve water samples were recovered. These are also indicated on the reflection amplitude and acoustic impedance versions of XLN 1160 (Figures 4 and 5).

The limit of the L-30 independent closure is mapped at two locations: to the west of the well at a time saddle, and to the northwest of the well where the trap becomes fault dependent (Figure 3). At Top Lower Missisauga level, the L-30 location is fully dependent on the fault trap to the north and the well is completely wet in this interval. Based on Sable analogues (Richards, 2008) it is likely that the two undrilled, fault dependent, footwall closures at Penobscot leak hydrocarbons upwards at cross-fault reservoir connections and any hydrocarbon columns are controlled by the extent of reservoir to non-reservoir juxtapositions at the bounding faults.

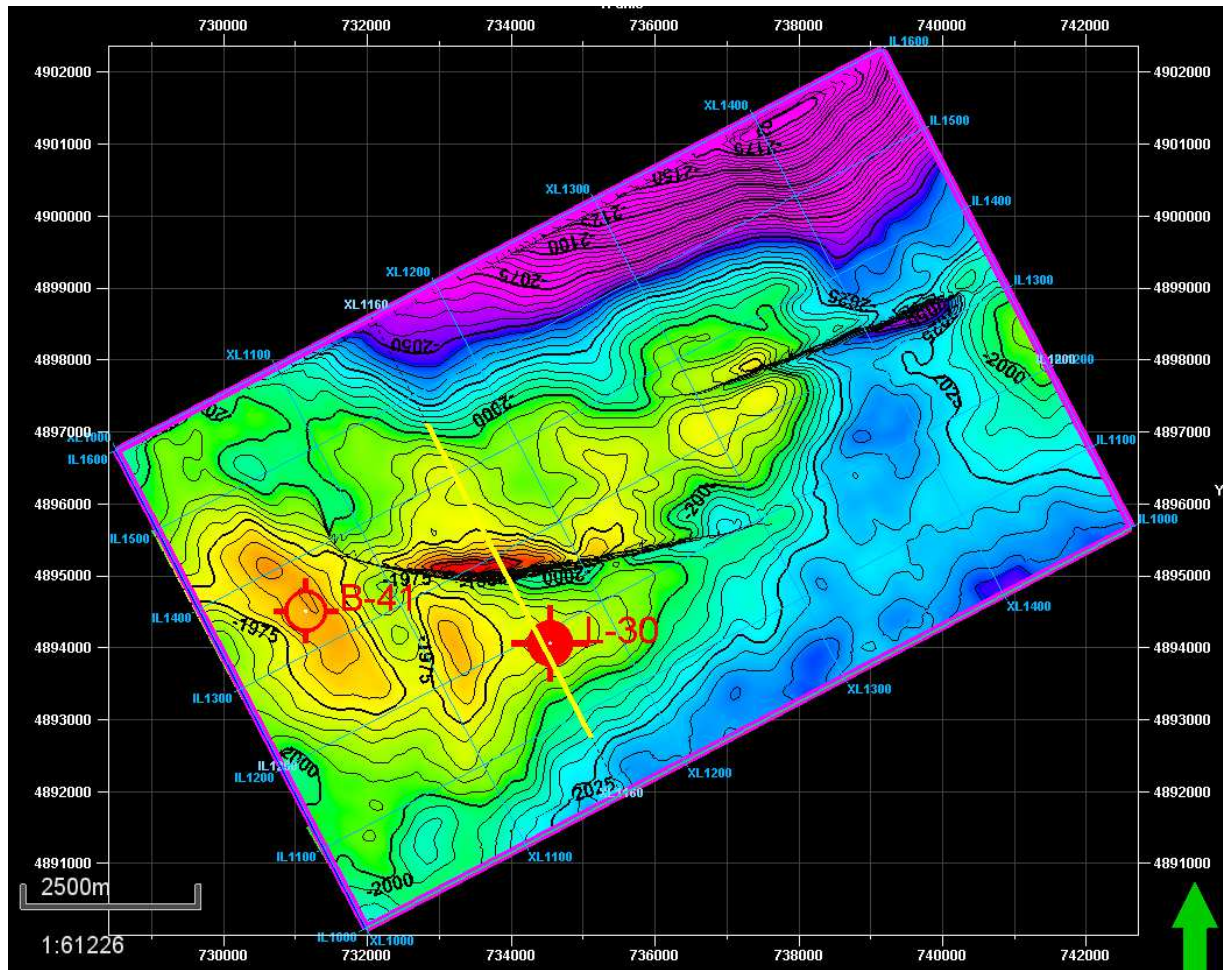


Figure 3: Top Middle Mississauga Two Way Time Structure (msecs). Top Middle Mississauga is the Red horizon at approximately 2000 msec in Figure 4. Yellow Line = XLN 1160 shown in Figure 4 and 5.

A full suite of well reports, wireline data, core data, velocity data, pressure data, formation tops and lithological logs is available for both wells from CNSOPB and GSC repositories. Two cores from Penobscot L-30 (from the Abenaki Formation) are described in Eliuk et al., 2008. Robertson Research International Ltd, 2000 (available upon request from CNSOPB) described four cores from Penobscot B-41 (from the Middle and Lower Mississauga are. Canstrat Ltd donated digital lithological logs to the Basin and Reservoir Laboratory,

Department of Earth Sciences, Dalhousie University. Divestco donated digital wireline data and well reports to the Basin and Reservoir Laboratory.

ACCEPTED MANUSCRIPT

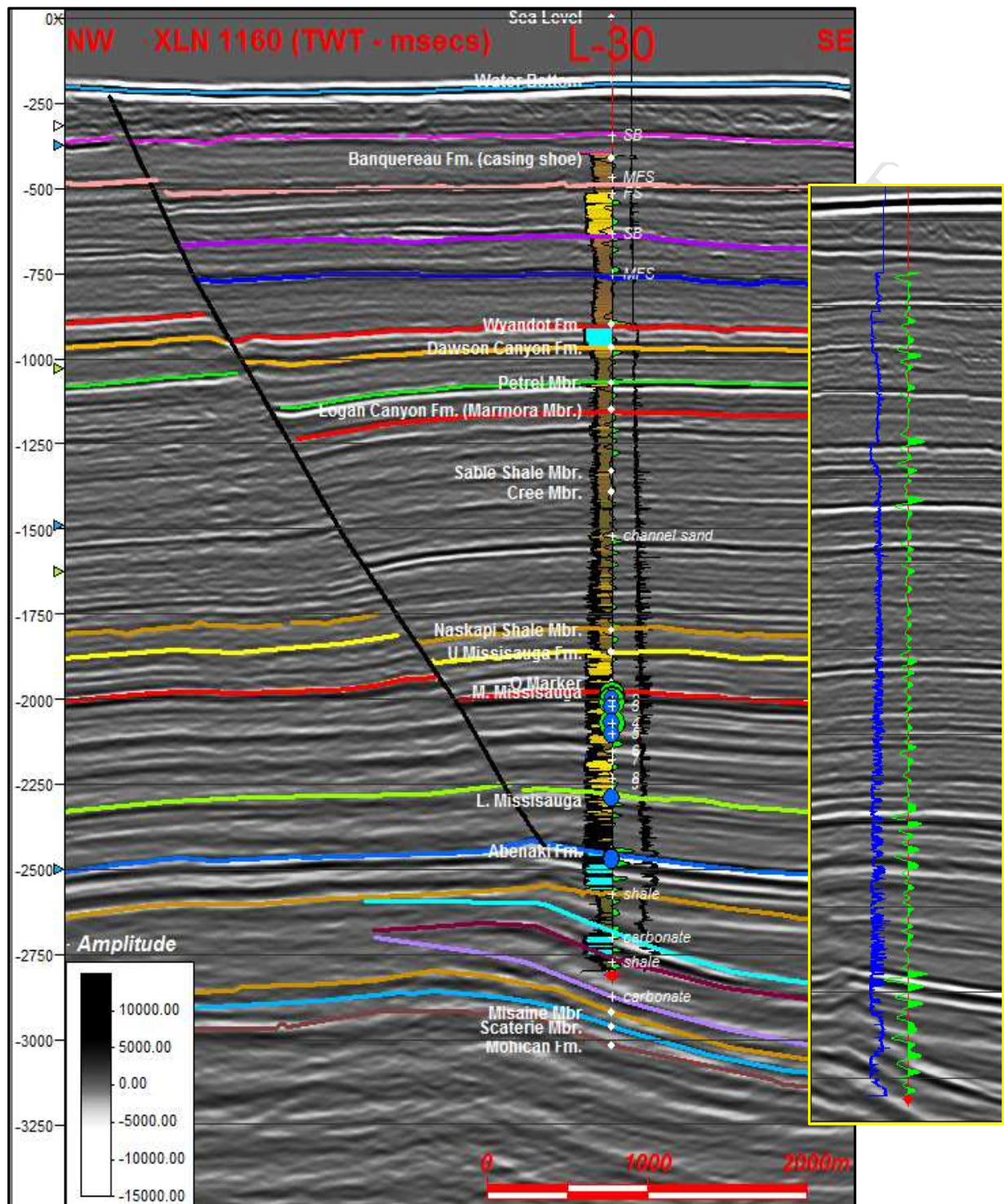


Figure 4: 3D XLN 1160. Seismic reflection data through Penobscot L-30 well (TWT msecs). Map in Figure 3 is the Red Horizon at approximately 2000msecs (Top Middle Missisauga). Gamma ray log (with lithology fill) is to the left of well trace. Synthetic seismic trace (green) is at the well. Acoustic impedance well log to right of well trace

(black). Stratigraphic markers to left of well. Annotations to right are referenced in text. Green circles = hydrocarbon RFTs, blue circles = water RFTs. Insert shows synthetic tie and Gamma ray log on XLN 1164 (exact location).

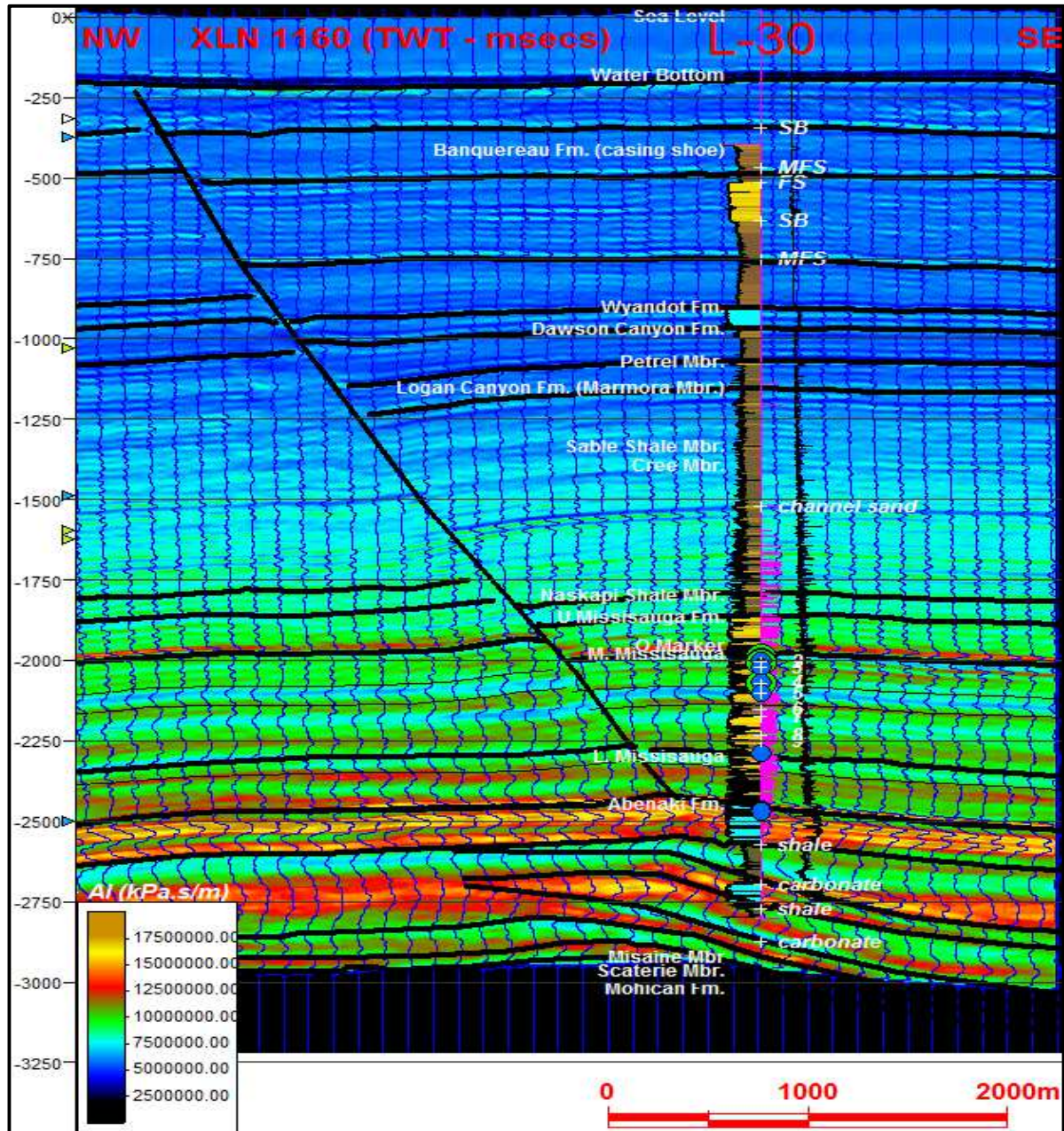


Figure 5: 3D XLN 1160. Acoustic impedance data through Penobscot L-30 well (TWT msec). Acoustic impedance is displayed as colour variable density format and ‘wiggle trace’ (blue) every 10 traces. Gamma ray log to left of well trace (with lithology fill). Density and porosity curves to right of well (purple). Acoustic impedance well log to

right of well trace (black). Stratigraphic markers to left of well. Annotations to right are referenced in text. Green circles =hydrocarbon RFTs, blue circles = water RFTs.

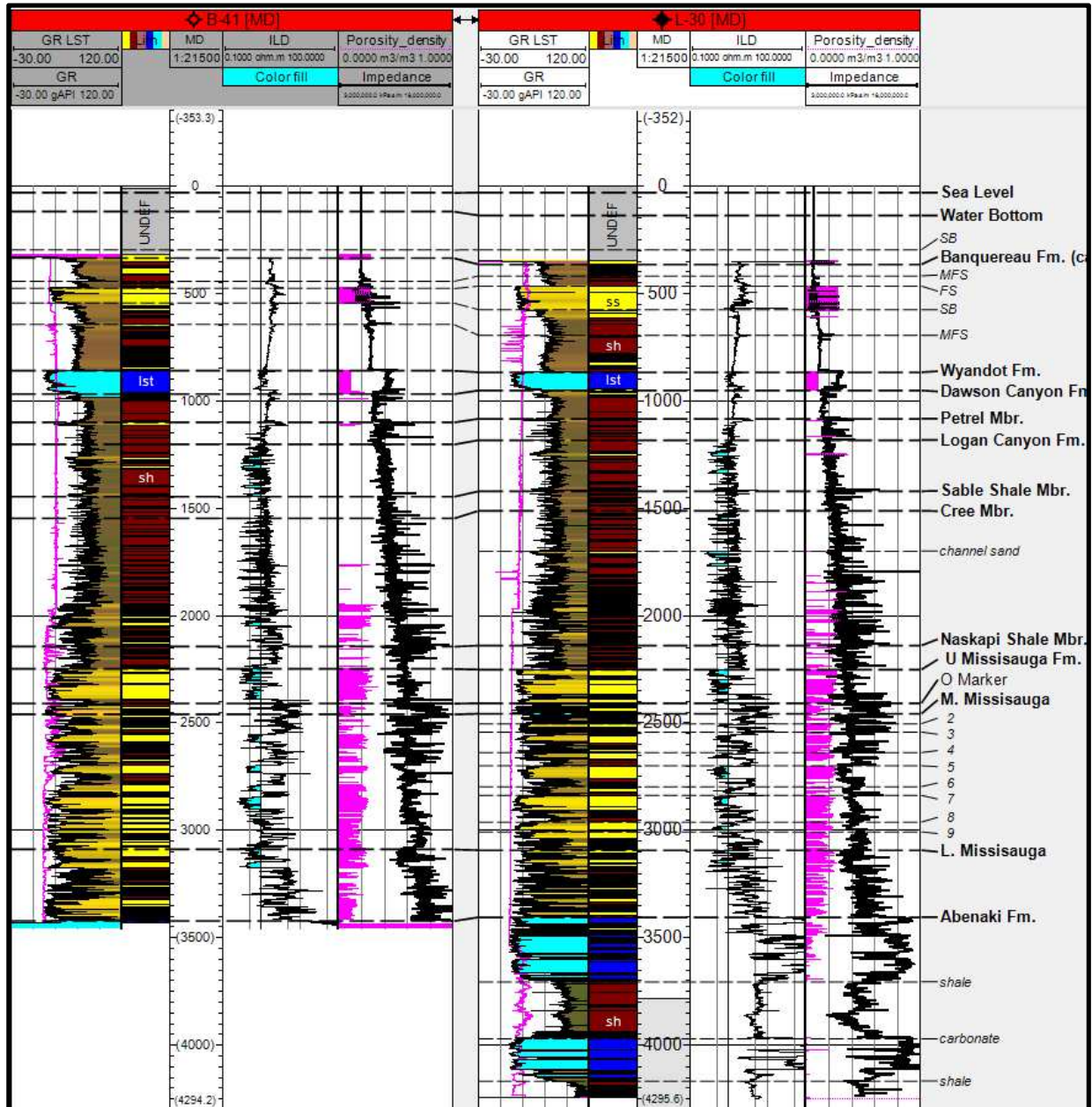


Figure 6: Well cross-section (MD m) Penobscot B-41 and L-30. Displaying the gamma ray (with lithology fill), CanStrat, Deep Resistivity, Density, Porosity (Purple) and Acoustic Impedance ($3-18 \times 10^6$ kPa.s/m). Main

stratigraphic markers are bold. Both wells are near vertical with KB=30.2m. Density logs are not available above Dawson Canyon: density porosities are ‘placeholders’).

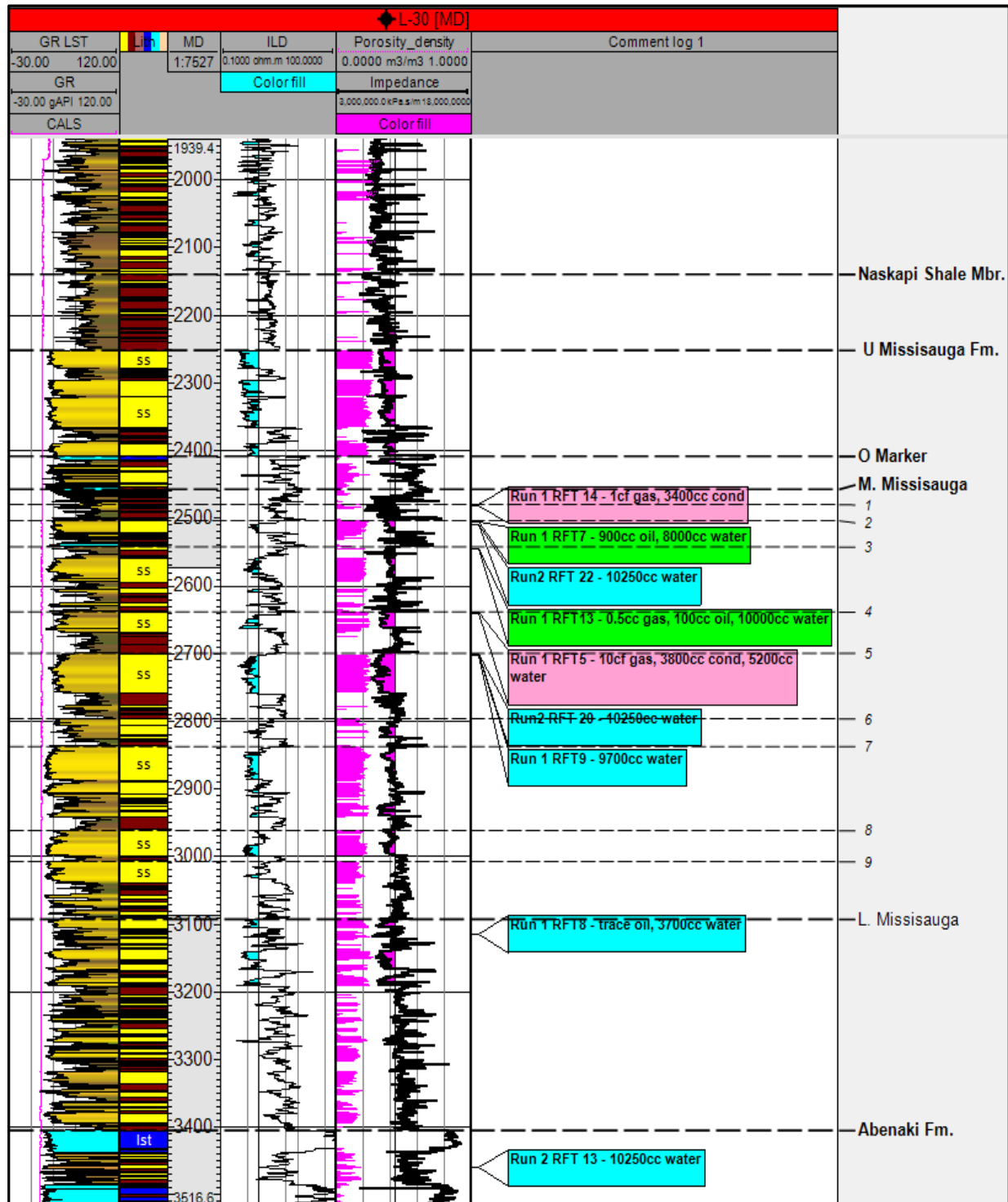


Figure 7: Missisauga Formation: detailed well log cross-section (MD m) Penobscot L-30 well. Displaying Gamma ray (with lithology fill), CanStrat, Deep Resistivity, Density Porosity (purple), Acoustic Impedance Logs and RFTs. Both wells are near vertical with KB=30.2m. Purple color fill on acoustic impedance log shows low impedance reservoir sands (<9,500,000 kPa.s/m).

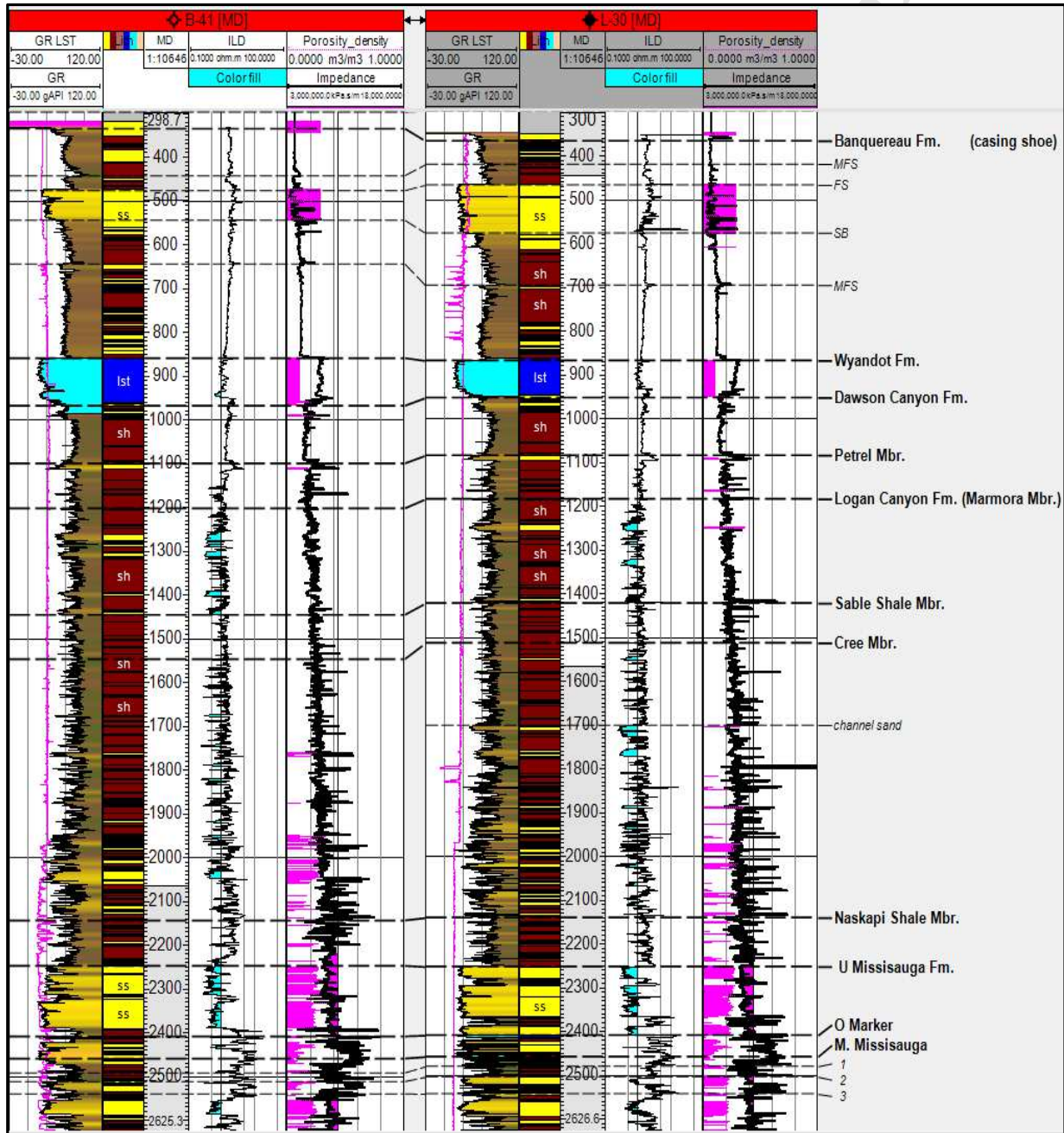


Figure 8: Detailed well log cross-section (MD m) of Banquereau, Wyandot, Dawson Canyon and Logan Canyon Formations. Penobscot B-41 and L-30 wells. Displaying Gamma Ray (with lithology fill), Canstrat, Deep Resistivity and Acoustic Impedance Logs. SB, FS, MFS = possible sequence boundaries, flooding surfaces & maximum flooding surfaces). Both wells are near vertical with KB=30.2m. Density logs are not available above Dawson Canyon density porosities are ‘placeholders’.

3.2. Penobscot 3D seismic survey

Nova Scotia Resources Ltd. acquired the Penobscot 3D marine seismic survey in 1991. The survey is now owned by the province and available through the CNSOPB and the Nova Scotia Department of Energy who have contributed the data set to the Open Seismic Repository ‘OpendTect’ (<https://opendtect.org/osr/pmwiki.php/Main/PENOBCOT3DSABLEISLAND>). The ‘OpendTect’ dataset also includes horizon data and well log data that were incorporated into this study.

The survey is nominally 7.2 km long and 12.03 km wide with a total area 86.62 km^2 (Figure 1). The area with live traces is slightly smaller. The inline range is from 1000 to 1600, the crossline range is 1000 to 1481 and the TWT range is 0 to 6000 milliseconds. The survey has a high signal-to-noise ratio and a bandwidth of ~10-60 Hz.

3.3. Seismic Interpretation (Petrel™ E&P Software Platform & Jason™ Software Suite)

The Penobscot 3D seismic, well, and horizon database was imported into both the Petrel™ E&P Software Platform and the Jason™ Software Suite. Schlumberger and CGG respectively donated these proprietary platforms to the Basin and Reservoir Laboratory, Department of Earth Sciences, Dalhousie University.

Both software platforms have extensive functionality. Petrel was used to perform structural, stratigraphic and seismic attribute interpretations on both reflection and impedance data. The focus in the Jason software was on seismic inversion. Of necessity, some functions, notably well-to-seismic ties, were performed on both platforms. Inverted 3D cubes were transferred from Jason to Petrel, with some iteration, to utilise volume attribute and flattening functionality.

Well-to-seismic ties, stratigraphic correlations between the wells, horizon and fault interpretations and time structure mapping are all straightforward at Penobscot and the interpretations performed here (Figures 3-8) are consistent with publicly available interpretations. Failure of the B-41 well suggests that time-to-depth conversion of low relief time structures is difficult to achieve accurately (partially due to the velocity effects of seabed topography and near-surface canyons).

Seismic to well ties are excellent using a 25-Hertz Ricker wavelet (e.g. Figure 4). Many reflections are amenable to 2-D or 3-D autotracking with appropriate ‘seed-picking’. Apart from some shallow splays the two main faults are readily interpretable in the clastic section above the carbonate hinge line. On the northeast margin of the Abenaki Carbonate Bank, limited well control and partially resolved inter-fingering of carbonate and clastic intervals introduce some interpretation uncertainty. The interpretation shown here (Figure 3) is based on projection of inboard wells, and a depositional model published by Wiesenberger (2000).

3.3. Seismic Inversion (Jason™ Software Suite)

The InverTracePlus™ module in the Jason Software Suite was used to perform a constrained sparse spike inversion on the Penobscot 3D cube. The workflow was as follows.

1. Five seismic horizons were imported from OpendTect: Water Bottom, Top Wyandot, Petrel, ‘O’ Marker and Top Abenaki (Baccaro Member). As this study was a test case aimed at evaluating this inversion technique in this area the horizon framework was deliberately conservative avoiding subjective interpretations based on regional stratigraphic models.
2. Well-to-seismic ties were established at L-30 and B-41 using a 25-Hertz Ricker wavelet and the imported seismic horizons were checked. These and multiple other horizons were also independently interpreted in Petrel.
3. The appropriate wavelet for inversion was determined by an automated model-driven process in which the forward model at each well is repeated, adjusting the wavelet each time, until the optimum match of the synthetic trace and real trace is accomplished. The ‘refined’ wavelet combining results at both wells has a 45° phase shift (Figure 9).

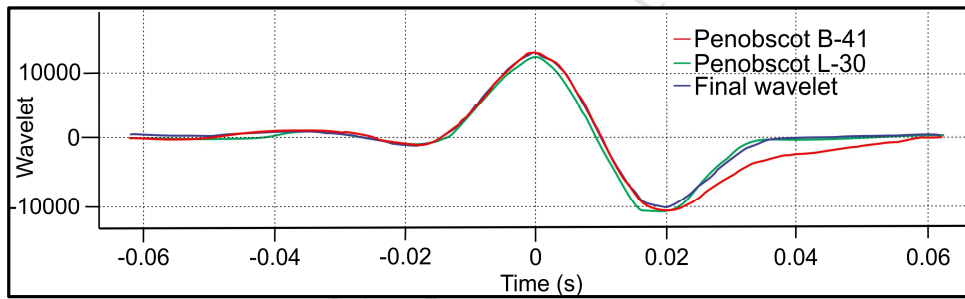


Figure 9: Estimated wavelets for L-30 and B-41 wells and final ‘refined’ wavelet for inverse modeling.

4. The imported seismic horizons were used to establish a framework throughout the 3D seismic cube. This is the ‘solid model’ (Figure 10). The water layer in the solid model was input by adding a horizon 200 milliseconds above the Water Bottom Horizon and the Abenaki layer by adding a horizon 500 milliseconds below the Abenaki / Baccaro Horizon.

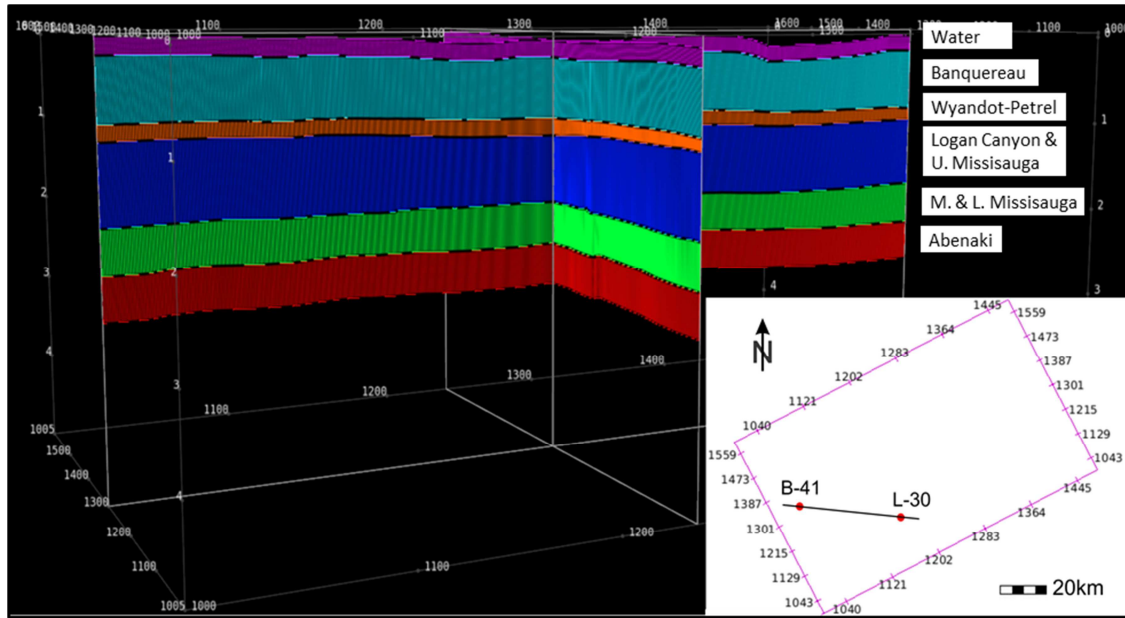


Figure 10: Penobscot Solid Model

5. An ‘a priori’ acoustic impedance model was then propagated throughout the solid model based on the wells. A low frequency model was also derived from the wells.
6. The inversion was then executed, by implementing an iterative forward modeling process, which converges on an optimum impedance solution at each seismic trace in the 3D cube. The result was inspected and exported to Petrel.

4. Results and Discussion

The results of these reflection-based and impedance-based interpretations at Penobscot are presented and discussed here, initially centred on the 3D dip-line through the L-30 well (XLN 1160). The reflection amplitude display of this line is Figure 4. The acoustic impedance display is Figure 5. Additional horizon-slice, attribute and vertical section displays are incorporated in the course of this discussion. The well-to-seismic ties are discussed and then the

major seismic horizons, seismic facies and lithologies are discussed referencing both cubes, considering the Sea-Bed to Base Cenozoic interval first, and followed by the Wyandot and Dawson Canyon interval, the Logan Canyon Formation, the Missisauga Formation and the Abenaki Formation.

It should be emphasised that because we are focussing on lithology prediction from absolute acoustic impedance, cross-sections and horizon slices are displayed as such - at a consistent colour scale. Adjusting colour scales can easily enhance subtle features, but that is not the primary intent here.

4.1. Well Ties

In Figure 4, the L-30 well tie to seismic amplitude data is established. A Gamma ray log (colour-filled by lithology), an acoustic impedance log, and formation tops are displayed in two-way-time (via the checkshot data), superimposed on the reflection amplitude data. The alignment of major log interfaces and formation tops with persistent high amplitude reflections indicates that the well data have been accurately positioned in two-way-time via checkshot data. This is supported by segmentation of the seismic section into zones of seismic character and facies that can be related to lithologies identified at the well and is confirmed by the synthetic seismogram displayed at the well (green ‘wiggle trace variable area’ display, WTVA, also shown as an inset). The B-41 well tie is of similar quality. The seismic reflection amplitude data are displayed in gray scale variable density format (VDF). Assuming zero-phase (and a polarity preference), each ‘hard kick’ (a downward increase in impedance- positive reflection coefficient) should be expressed by a black peak with associated side lobes, almost perfectly exemplified at the water bottom). Similarly, each ‘soft kick’ is a white trough with associated side lobes. Where positive

and negative reflections are closely spaced it is often difficult to interpret which intervals are high impedance and which intervals are low impedance on the reflection amplitude data, and this is a key driver for acoustic impedance inversion.

In Figure 5, the L-30 well tie to the acoustic impedance data is established. The acoustic impedance well log (black), to the right of the well, is carefully aligned with an acoustic impedance trace (blue) derived from the seismic data. From Abenaki to Wyandot there is a very close match between the acoustic impedance calculated at the well with the inversion of the seismic data. The match is poorer in the Banquereau section where the impedance cube has values that are a little high. Above the Dawson Canyon Formation no density log data are available and so densities have been estimated in the Wyandot and Banquereau Formations. Above the 16' casing shoe no well log data are available. The strategy in this study was to restrain input to the inversion to ‘hard’ well data and conservative horizon interpretations. A shallow pseudo-log could reasonably be utilized to extend the shallow well log impedance upwards to an acoustic impedance of 1,500,000 kPa.s/m in the water interval (water velocity ~1500 m/sec, water density ~1000 kg/m³) and this would improve the inversion in the shallow section. The synthetic seismogram trace shown in Figure 4 is replaced by a density-porosity display in Figure 5 (purple). In Figures 6, 7 and 8 well logs are shown in detail: in Figures 6 and 8, Wyandot and Banquereau density porosities are shown only as ‘placeholders’ (no density logs).

The acoustic impedance seismic cube is displayed in VDF with every 10th trace displayed as a blue WTVA trace. The colour scale ranges from ~4,000,000 kPa.s/m (dark blue) in low velocity (~2000m/sec), low density (~2000 kg/m³), unconsolidated clastics to values over

17,000,000 kPa.s/m (yellow and red) in tight Abenaki carbonates where velocities exceed 6500 m/sec and densities exceed 2650 kg/m³.

4.2 Water Bottom – Base Cenozoic

This interval is bounded by two major ‘hard kicks’: at the water bottom and at Top Wyandot Formation. Well logs are shown in detail in Figure 8. Acoustic impedance values are typically in the range 5,000,000 - 8,000,000 kPa.s/m (medium – light blue). No ‘bright spots’ (low impedance) typical of shallow gas sands are evident. Acquisition artifacts contaminate the data and are evident in horizon-slices as well multiples from shallow canyons.

A low reflectivity ‘transparent’ interval immediately above the Wyandot (Base Cenozoic) ties to a shale interval at the L-30 well (Figure 4). Within this shale a high amplitude MFS (maximum flooding surface) marks a change from deepening to shallowing, based on the gamma ray signature. A sandy interval immediately above in the L-30 well is bounded by strong reflections, probably a sequence boundary (SB) at its base with moderate amplitude continuous internal reflections. This is overlain by second transparent shale with an MFS near its base at the well, in turn overlain by a second high amplitude interval to the water bottom, probably a sandy interval with an erosional base, but with shingled less continuous reflectivity.

Two key features are evident on timeslices and horizon-slices through the Cenozoic section: shallow canyons immediately below the seabed and polygonal fracture systems at Base Cenozoic / Top Wyandot. A canyon on the east side of the cube (not penetrated at the L-30 well) is illustrated in Figures 11a and 11b. This canyon cuts down from the water bottom at approximately -250msecs to approximately -600msecs. Multiples from this canyon contaminate deeper timeslices including the Wyandot horizon-slice shown in Figure 12a. There is also

contamination from a second seabed canyon on this Wyandot horizon-slice, just east of the B-41 well. This western canyon is shown in the middle to upper left of XLN 1090, Figure 12b and in map-view overlies the Top Middle Missisauga time saddle (Figure 3) that separates the B-41 time closure from the ‘leaky’ faulted closure immediately to the east. Despite undershooting, the velocity effects of these canyons probably contribute to inaccuracies in time-to-depth conversion of deeper reflections.

Wyandot polygonal fracturing at the base of the Cenozoic is illustrated by horizon-slices and in section-view in Figures 12a and 12b. Smoothing the Wyandot horizon and then flattening the reflection amplitude and acoustic impedance cubes constructed these horizon-slices. Scrolling these flattened cubes up and down indicates that this fracture pattern terminates ~20 msec above, and ~40 msec below the Top Wyandot horizon (indicated in Figure 12b). For clarity: timeslices are horizontal slices through the seismic cube with no adjustment for structure; horizon-slices are horizontal slices through the cube after flattening on a seismic horizon. Timeslices cut across stratigraphy unless there is no dip, horizon-slices are intended to be images at discrete stratigraphic levels.

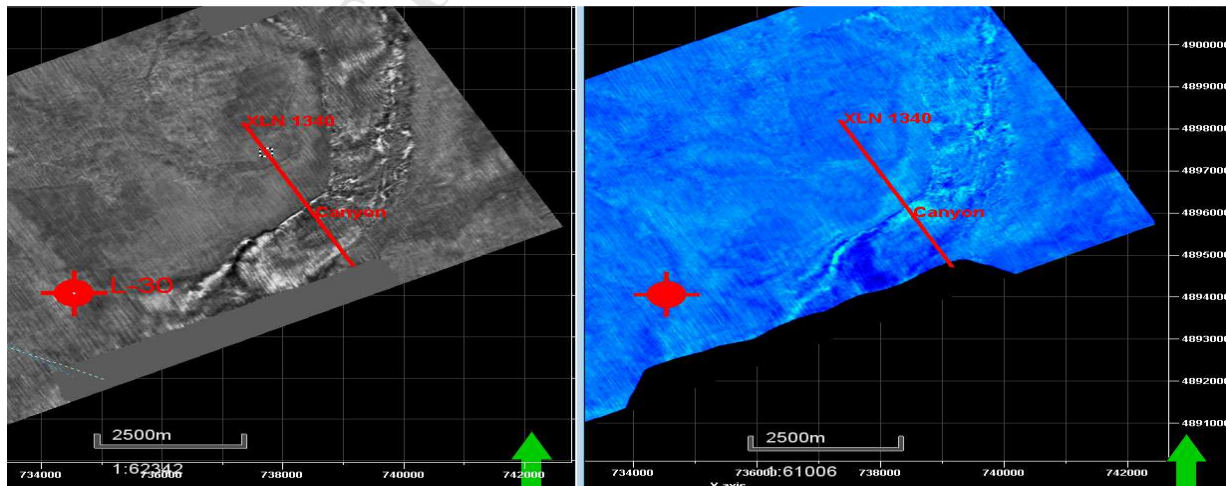


Figure 11a: Reflection amplitude and acoustic impedance timeslices at 415 msecs below sea level showing a near-surface canyon. XLN 1340 (location) is shown in Figure 11b.

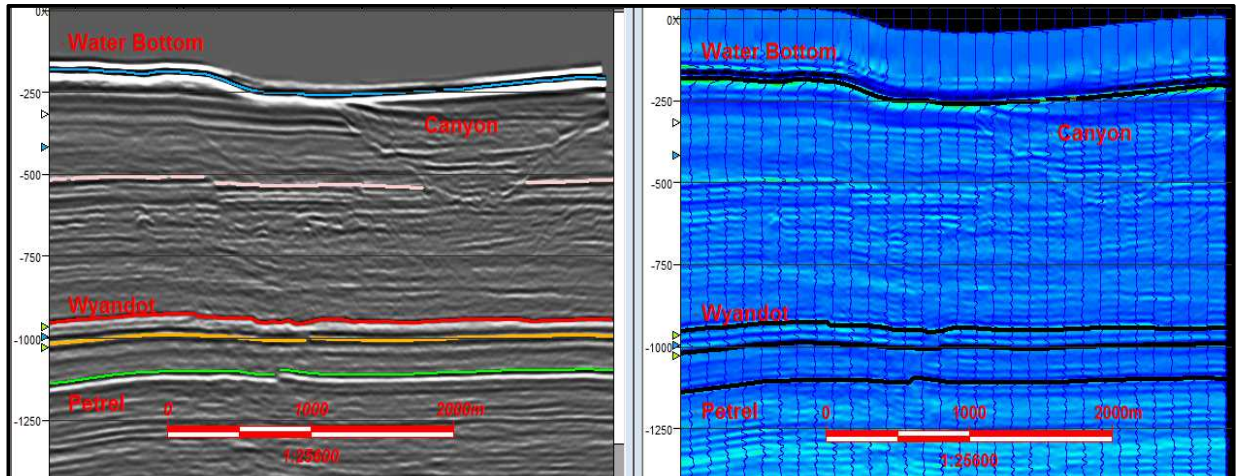


Figure 11b: XLN 1340 (TWT msecs) reflection amplitude and acoustic impedance sections. Canyon is located in the upper right. Location is in Figure 11a).

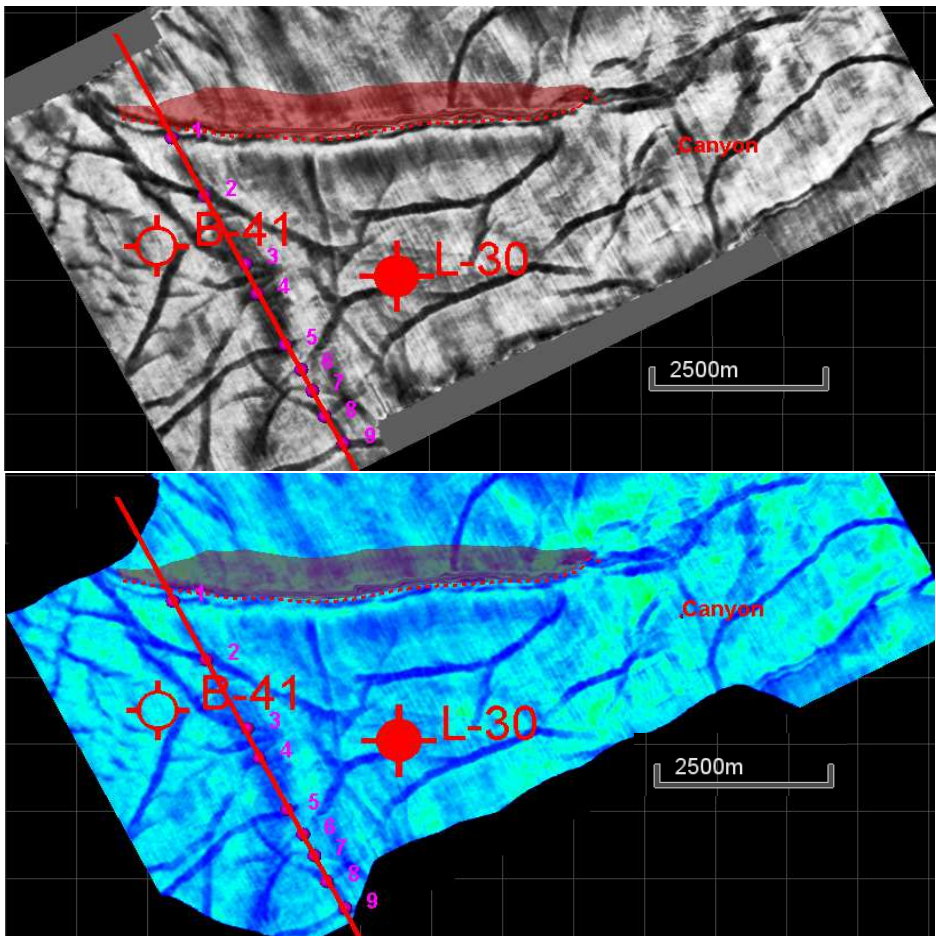


Figure 12a: Wyandot polygonal fracturing on reflection amplitude and acoustic impedance horizon-slices (cubes flattened on smoothed Wyandot horizon). Location of XLN 1090 is shown. Specific cracks are labelled 1-9, to reference Figure 12b (XLN 1090). Transparent red polygons are mapped faults that extend down to base clastic section. Acquisition artifacts and ‘shadows’ from two near seabed canyons are evident in these slices. Slow velocities in the near seabed canyon east of B-41 may contribute to the failure of the B-41 time structure as a hydrocarbon trap.

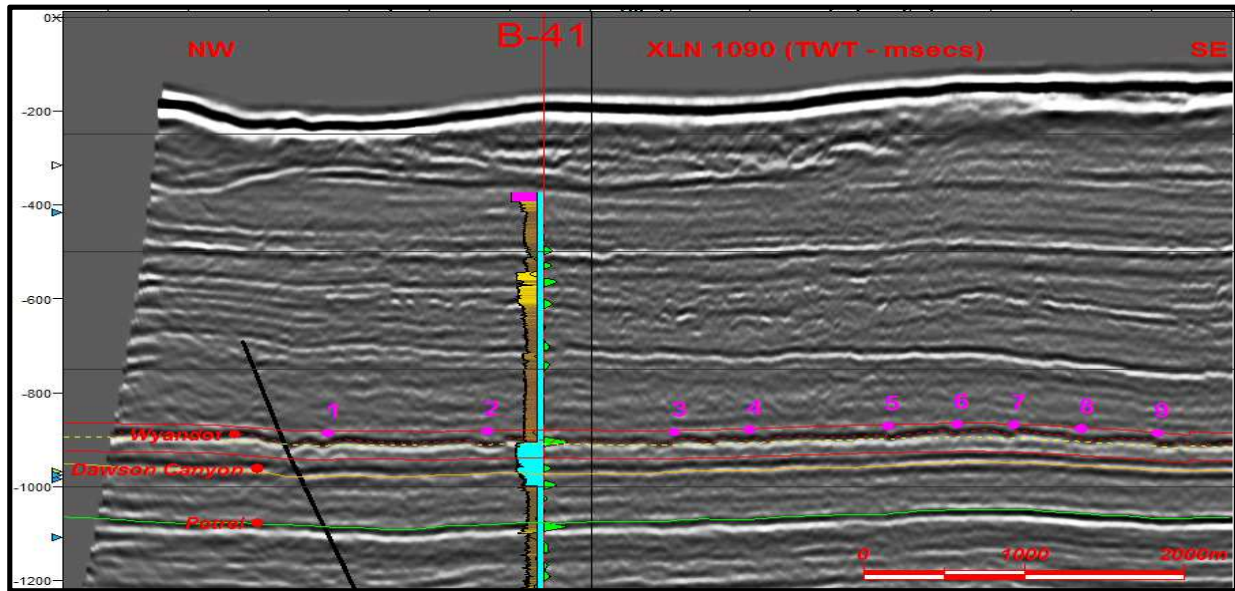


Figure 12b: XLN 1090 (TWT msecs). Structural section showing Wyandot polygonal features in section-view: labelled 1-9, referenced to horizon-slices. B-41 well is projected 1800 m and time-shifted. Dotted red line is original Wyandot horizon; dashed yellow is smoothed Wyandot horizon at level of horizon-slices in Figure 12a. Solid red horizons are upper and lower limits of polygonal fracturing on horizon slices in flattened cube.

4.3 Wyandot and Dawson Canyon Formations

The Wyandot is bounded at its top by the Base Cenozoic ‘hard kick’ discussed above and at its base by a strong trough ‘soft kick’ from the more gradational basal interface with Dawson Canyon Shale (Figure 4). On the impedance cube, Wyandot impedances (light blue-green) exceed 7,000,000 kPa.s/m (velocity ~3000 ms/sec, density ~2300 kg/m³) and stand out from a shale background (medium blue) of ~ 5,000,000 kPa.s/m (velocity ~2200 ms/sec, density ~2200 kg/m³). The Top Dawson Canyon reflection and the reflection from the Petrel Member (a thin chalk within the Dawson Canyon) are separated by a ‘transparent’ shale interval and are two of

the most persistent, conformable, seismic markers throughout the Sable sub-Basin. These provide excellent datums for flattened cubes.

4.3 Logan Canyon Formation

The top of the Logan Canyon Formation is typically not interpreted directly as it is close to the regional Petrel seismic marker and can be readily mapped via an isochron. The Logan Canyon Formation increases in reflectivity and acoustic impedance downwards (Figures 4 and 5) reflecting compaction and increasing sand content / thickness. It is not immediately obvious in cross-section view, but when timeslices and horizon-slices are viewed in the Logan Canyon there is an abundance of channels and channel complexes in this section. Figures 13a, b, c and d are a selection of the many horizontal slices in the Logan Canyon that display these coastal plain / shallow marine channels. In cross section view these abundant narrow channels give the reflection amplitude data a ‘speckled’ appearance (or seismic facies).

A single Logan Canyon channel, approximately 20 m thick and 1000 m wide, is penetrated at the L-30 well. Well logs through this channel are shown in detail in Figure 8 (channel at ~1700 m MD). On XLN 1160 (Figure 4) the reflections associated with this channel, just below 1500 msec, do not appear confined because the seismic section is aligned with the thalweg of the channel (NNW-SSE). This channel is shown in horizon-slice view in Figure 13d and in an orthogonal vertical section in Figure 14 (ILN 1185), where a second, much narrower channel ~100m wide, is evident to the northeast.

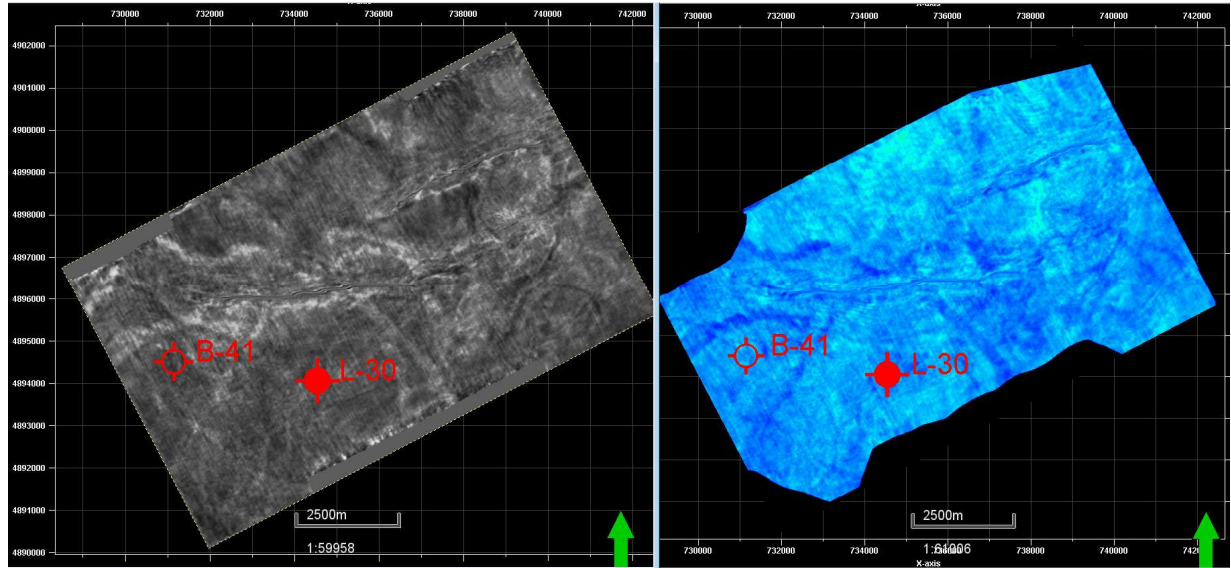


Figure 13a: Reflection Amplitude and Acoustic Impedance horizon-slices 100 msecs below Petrel horizon.

Meandering channels (low impedance) are evident approximately 500 m north and 2500 m north of B-41 and approximately 2500m east of L-30. These are the first channels in the Logan Canyon evident below the Petrel Horizon.

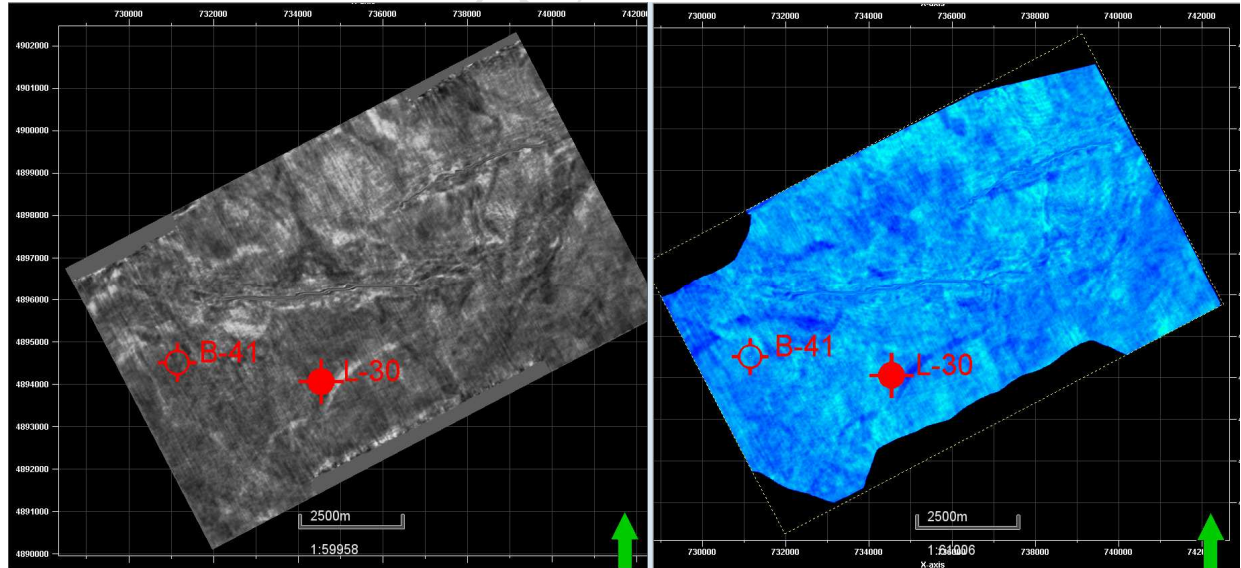


Figure 13b: Reflection Amplitude and Acoustic Impedance horizon-slices 108 msecs below Petrel horizon.

Meandering channels (low impedance) are evident approximately 500 m north of B-41 and just east of L-30.

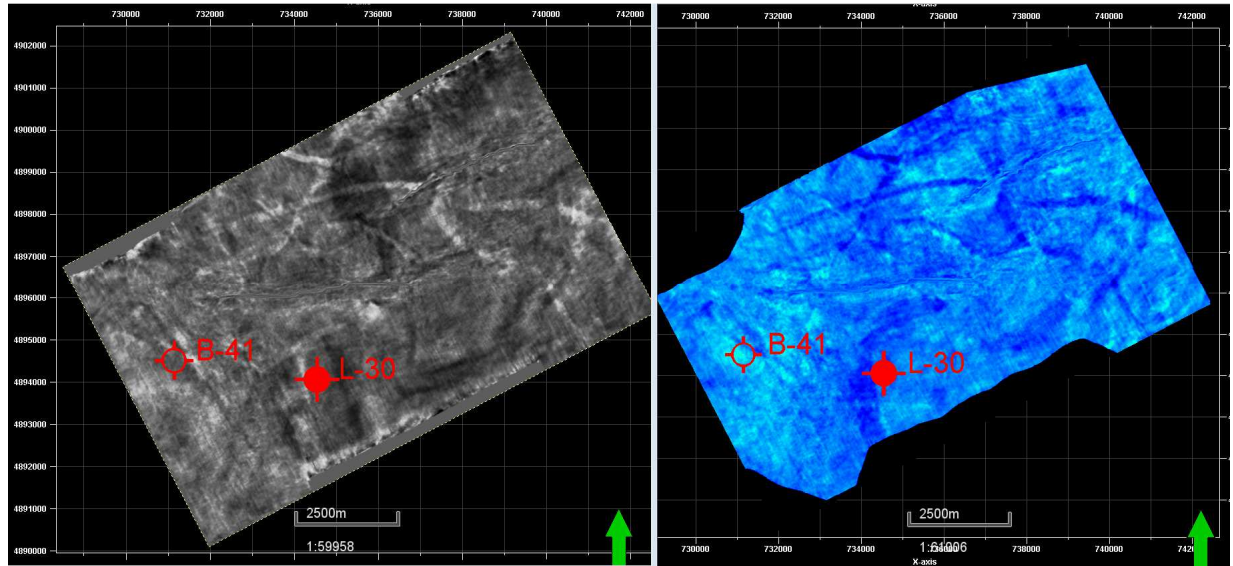


Figure 13c: Reflection Amplitude and Acoustic Impedance horizon-slices 200 msecs below Petrel horizon.

Displaying multiple cross-cutting meandering and straight channels (low impedance).

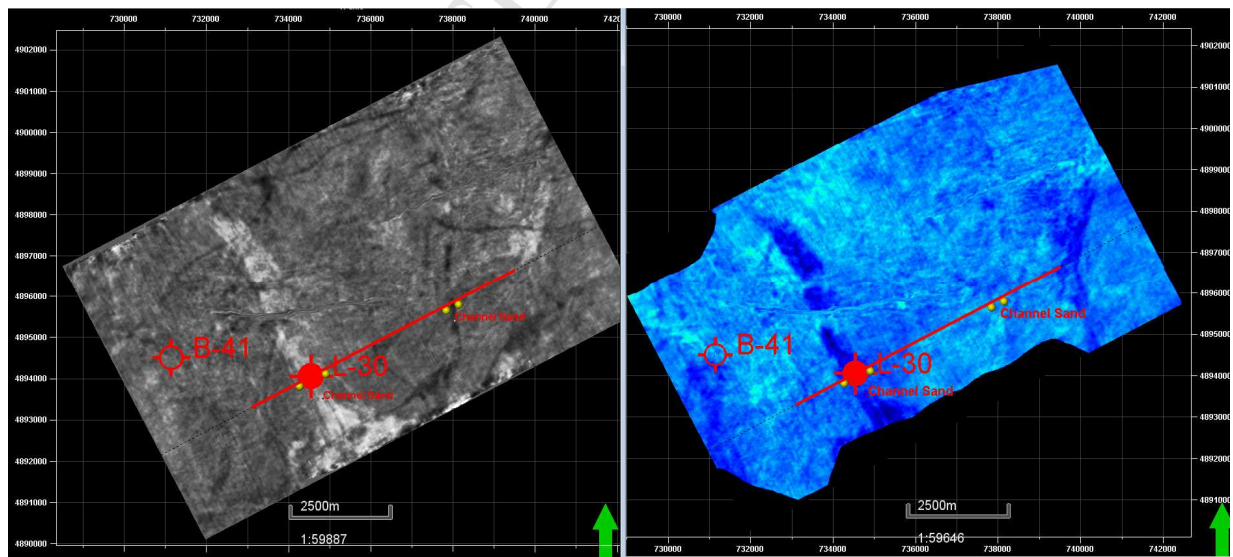


Figure 13d: Reflection Amplitude and Acoustic Impedance horizon-slices 450 msecs below Petrel horizon. The red line is ILN 1185 (Figure 14). A broad (1000 m) low impedance channel is penetrated at L-30 well (well logs Figures 6 and 8, labeled Figure ‘channel’ at 1700m MD). To the east there is a narrow (100m) slightly younger low impedance channel.

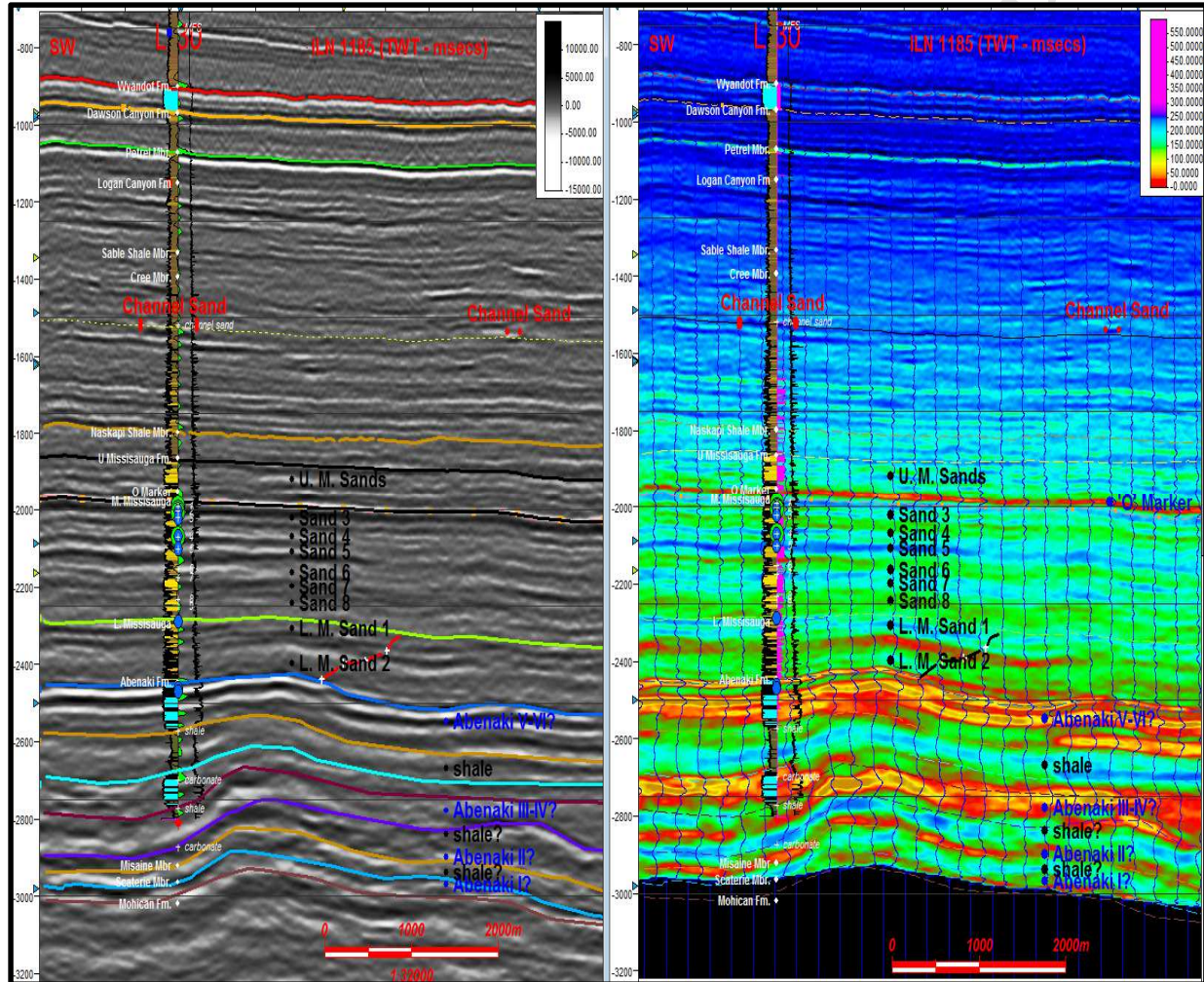


Figure 14: 3D ILN 1185 (TWT msecs) Reflection Amplitude and Acoustic Impedance. Location shown in Figure 13d. A Logan Canyon channel penetrated at the L-30 well is indicated just below 1500 msecs. The impedance log to right of well shows this low impedance sand is ~20 m thick. A second, slightly younger, narrow, channel is annotated to the northeast, slightly higher in the section relative to the level of the horizon slice (dashed yellow on amplitude section, black on impedance section). Low impedance reservoir sandstones in the Missisauga are

annotated. High impedance carbonates and low impedance shales are interpreted (speculatively) based on the stratigraphic model of Weissenberger, 2000).

4.4 Missisauga Formation

The Missisauga Formation is more compacted than the overlying Logan Canyon Formation and has a much higher net-to-gross ratio (Figure 14). This results in larger acoustic impedance contrasts and more cyclical high amplitude reflectivity. Reservoir sandstones are scaled blue (~7000, 000 kPa.s/m), tight sandstones and shales green, (~10,000,000 kPa.s/m), and the ‘O’ marker limestone red (~13,000,000 kPa.s/m). The key reservoir sandstones are annotated in Figure 14 consistent with the logs in Figure 7 and are easily correlated as low impedance intervals on impedance sections. Horizon-slices from two Upper Missisauga and three Middle Missisauga sandstones are shown as Figures 15a-15e. Some broad facies belts and a few confined channels are evident, but without sharp changes in lithology it is difficult to separate stratigraphic and lithological variations from subtle cross-cutting of stratigraphy and fault shadow effects that contaminate the horizon-slices. The Missisauga reservoir sandstones are clearly much thicker and more extensive areally than sandstones in the Logan Canyon Formation and a key point in showing these Missisauga slices is that they are relatively featureless compared to the Logan Canyon horizon-slices. This reflects the change in depositional setting described in Section 2.

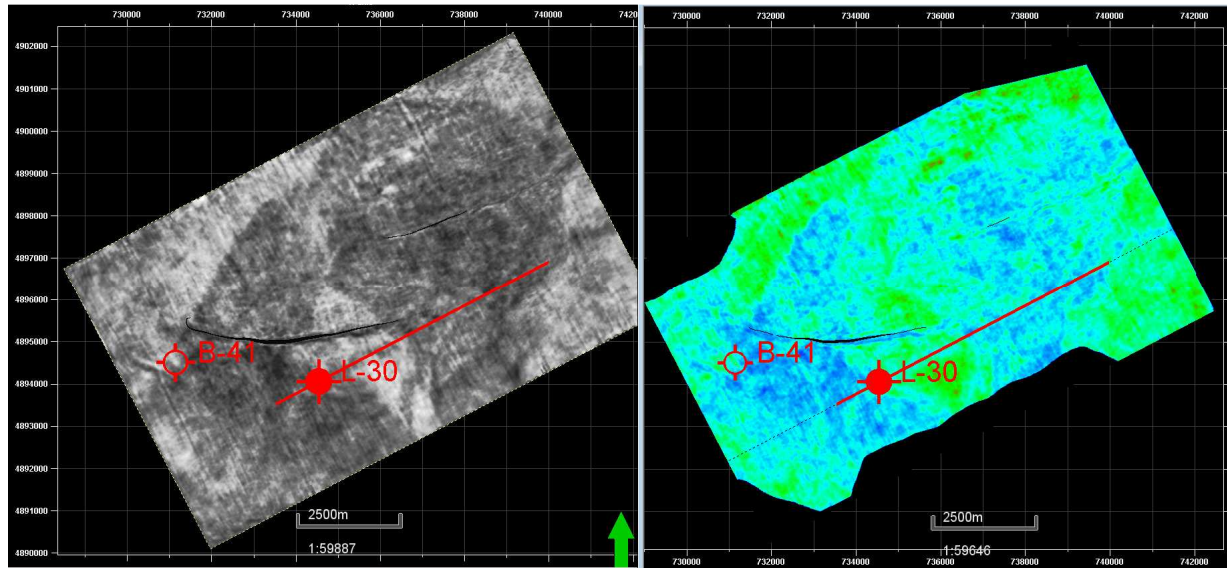


Figure 15a: Reflection Amplitude and Acoustic Impedance horizon-slices ~100 msecs above Top Middle Missisauga Horizon (Level of Top U.M. sands annotated in Figure14).

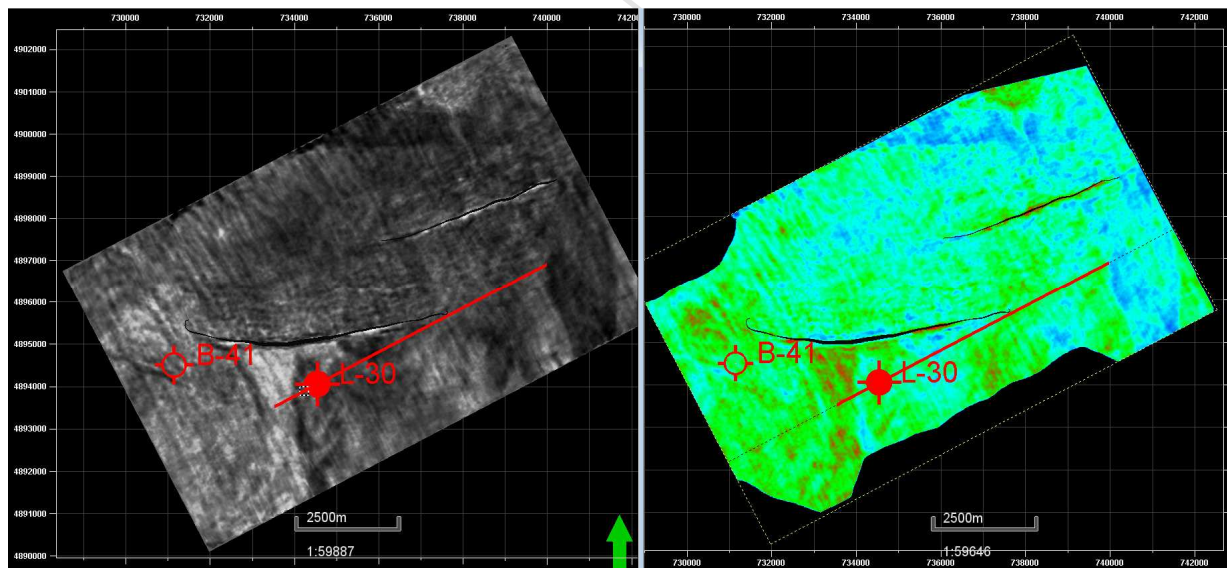


Figure 15b: Reflection Amplitude and Acoustic Impedance horizon-slices ~24 msecs above Top Middle Missisauga Horizon (Upper Middle (U.M) sands annotated in Figure 14).

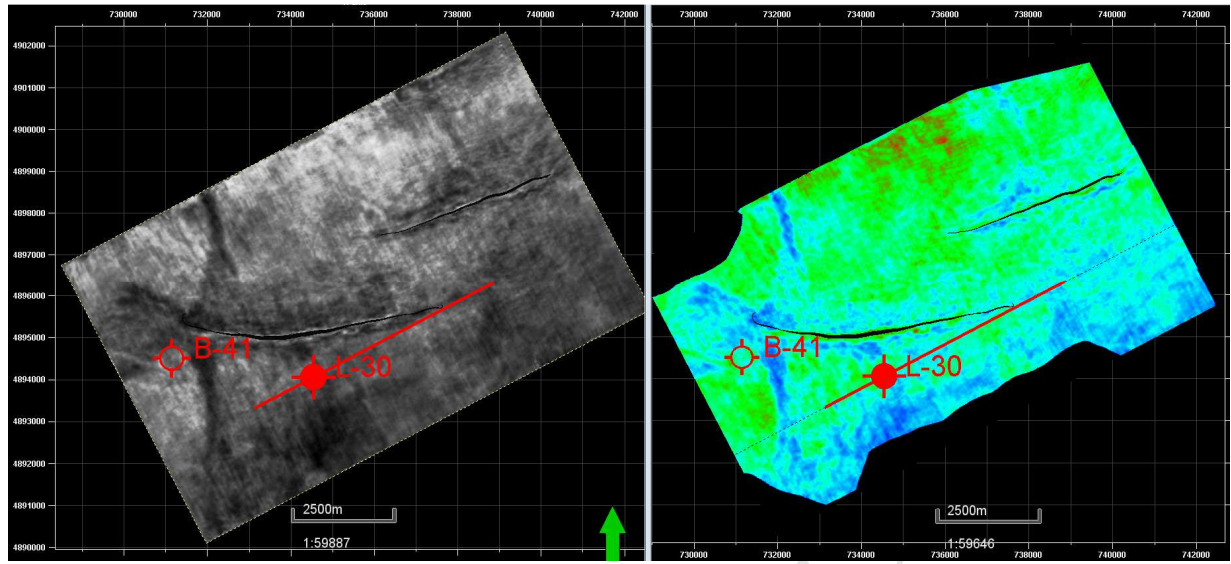


Figure 15c: Reflection Amplitude and Acoustic Impedance horizon-slices ~ 12 msecs below Top Middle Missisauga Horizon (Level of Sand 1 in Figure 14).

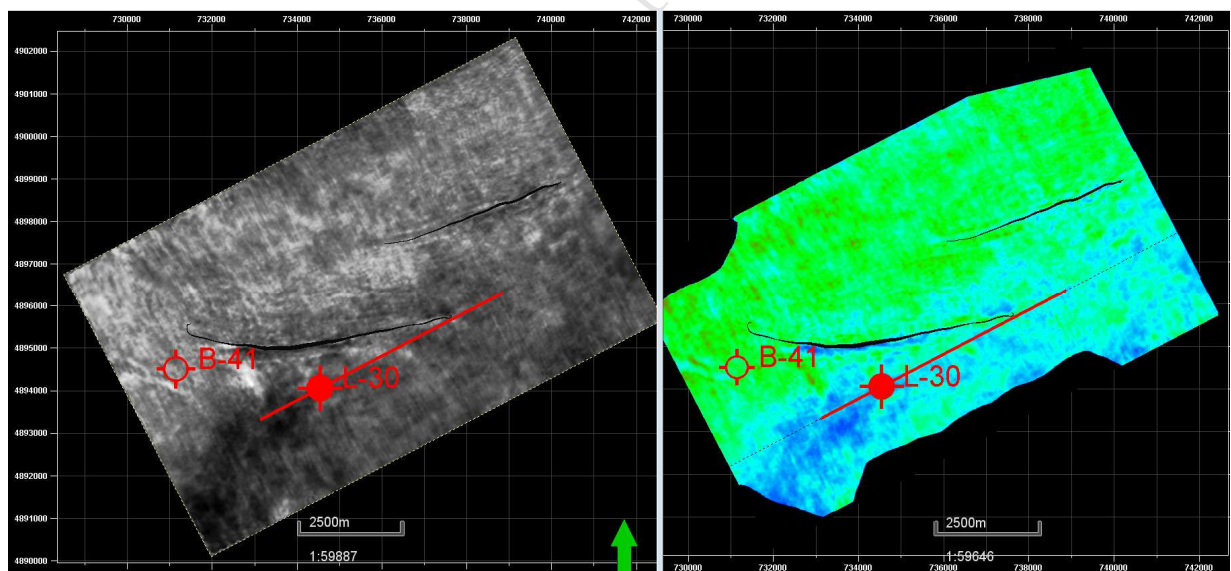


Figure 15d: Reflection Amplitude and Acoustic Impedance horizon-slices 95 msecs below Top Middle Missisauga Horizon (~Sand 4).

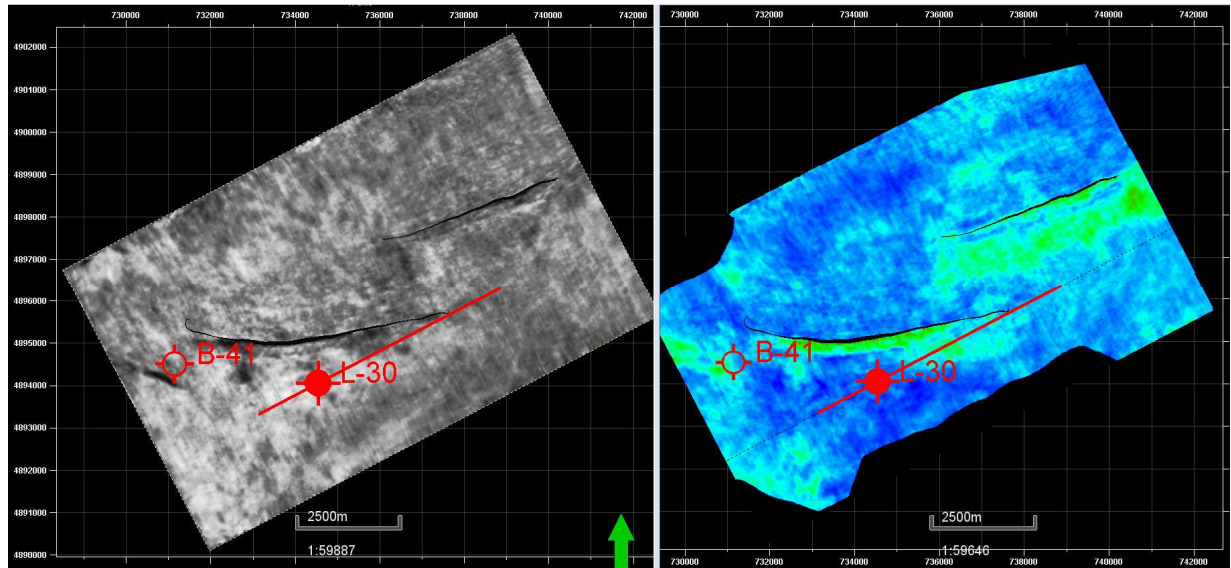


Figure 15e: Reflection Amplitude and Acoustic Impedance horizon-slices 150 msec below Top Middle Missisauga Horizon (~Sand 5).

4.4 Abenaki Formation

In keeping with a strategy of providing a conservatively interpreted horizon framework to the *a priori* model, only the Top Abenaki horizon (Figure 16a, XLN 1160) and a model base horizon were provided in this interval, together with acoustic impedance from the well penetrations. The B-41 well just ‘tags’ the top of the carbonate section, the L-30 well penetrated almost 300 m of Abenaki Formation (Baccaro Member) carbonate, followed by approximately 290 m of shale and a further 270 m of carbonate. There is an early interpretation in the GSC ‘BASIN’ data base, that this lower shale unit is the Misaine Member and that the lower carbonate is the Scaterie Member. These picks were subsequently revised, probably when it became clear from inboard drilling that L-30 had not penetrated the full Abenaki Formation.

The inversion result shown Figure 16b is therefore constrained by the formation top horizon, the reflection data and, essentially, impedance from the L-30 well only. The Abenaki Bank margin is rendered as a dipping interval of interfingering low impedance units (shales) and high impedance units (carbonates), both above and below the deepest penetration of the L-30 well. The associated interfaces are interpreted on the reflection amplitude section, but did not form part of the *a priori* model. This interfingering of siliciclastics and carbonates is consistent with a depositional model from the Panuke-Cohasset area, developed with dense well control and 3D data by Weissenberger et al. (2000).

To the west an inboard well, which fully penetrated the Abenaki Carbonate Bank, has been copied and projected 28 km into the Penobscot cube and time shifted so that the top of the carbonate interval at the well matches the top carbonate seismic horizon interpreted at Penobscot. This projected tie is also consistent with a high amplitude trough interpreted as the base of the Abenaki carbonate at Penobscot (without a well tie). The projected tie is shown in Figures 16a and 16b.

Based on this projected well tie, and the homogenous appearance of the amplitude data at the projected well, it is interpreted that this whole interval is massive high impedance carbonate and the low impedance shale projected from L-30 by the inversion is probably incorrect, indicating a limitation of the inversion, which could be fixed locally if there is sufficient well penetration and a detailed horizon framework is supplied. However, this rests on the assumption that the regionally based interpretation is correct. Shale incursions into carbonate banks usually have a proximal limit, but complete drowning can also occur. Alternate interpretations are possible: Sayers (2013) interprets the Abenaki Bank to be approximately 3 km wide with symmetrical interfingering of carbonate and shale on its southeast side below L-30 and its

northwest side nearby (identified in Figure 12 of Sayers, 2013). Qayyum (2014) interprets the Abenaki Bank similarly to here, but with *relative* impedance data the NW-SE line through the L-30 well in that study (Figure 4d in Qayyum, 2014) shows layering of low, moderate and high impedances with the carbonate bank interior.

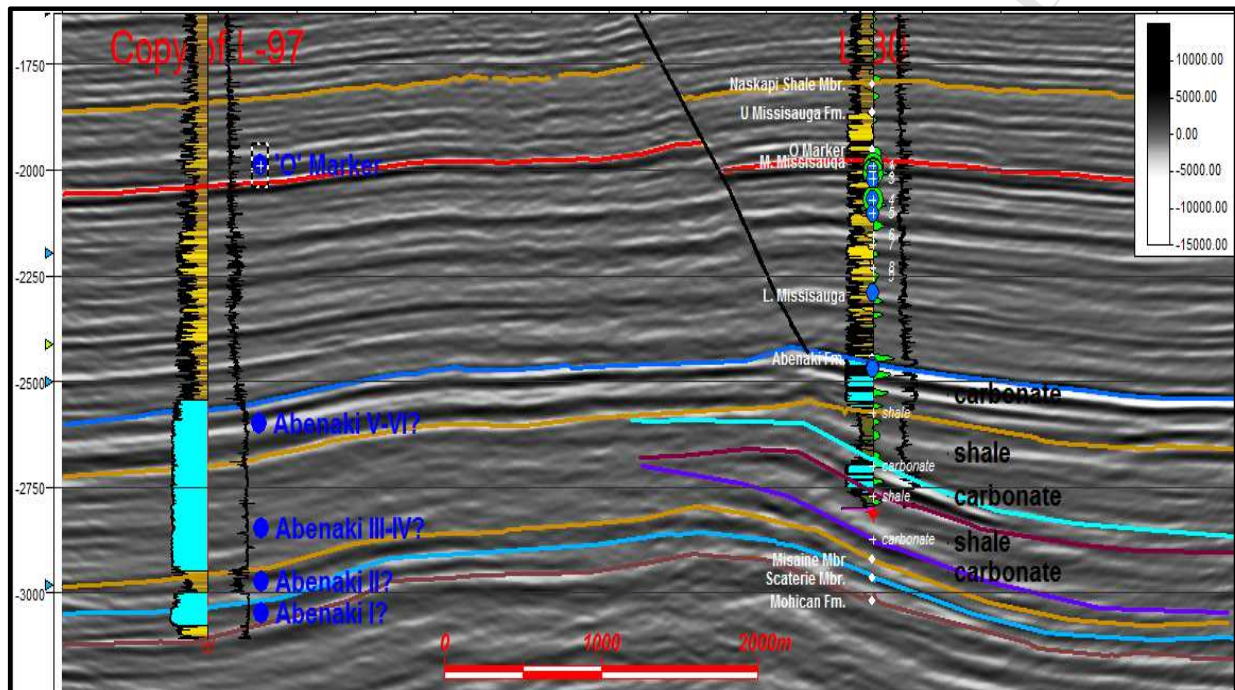


Figure 16a: Reflection Amplitude XLN 1160 (TWT msecs) with projected L-97 well tie.

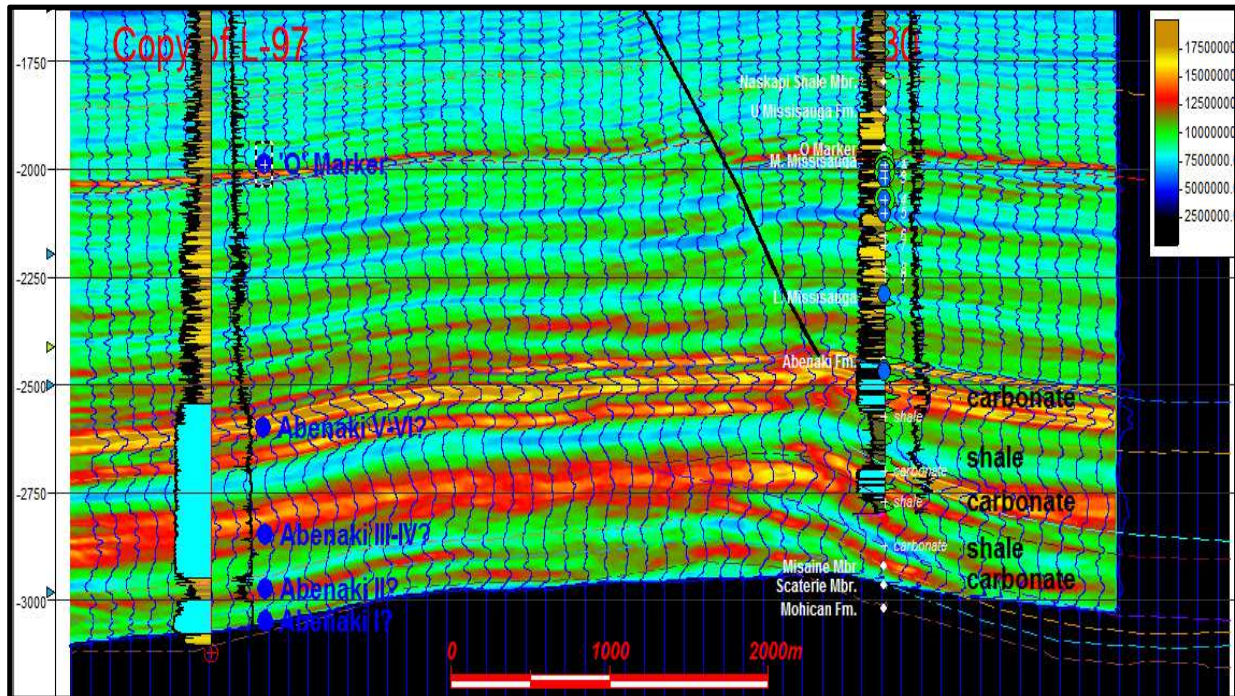


Figure 16b: Acoustic Impedance XLN 1160 (TWT msec) with projected L-97 well tie.

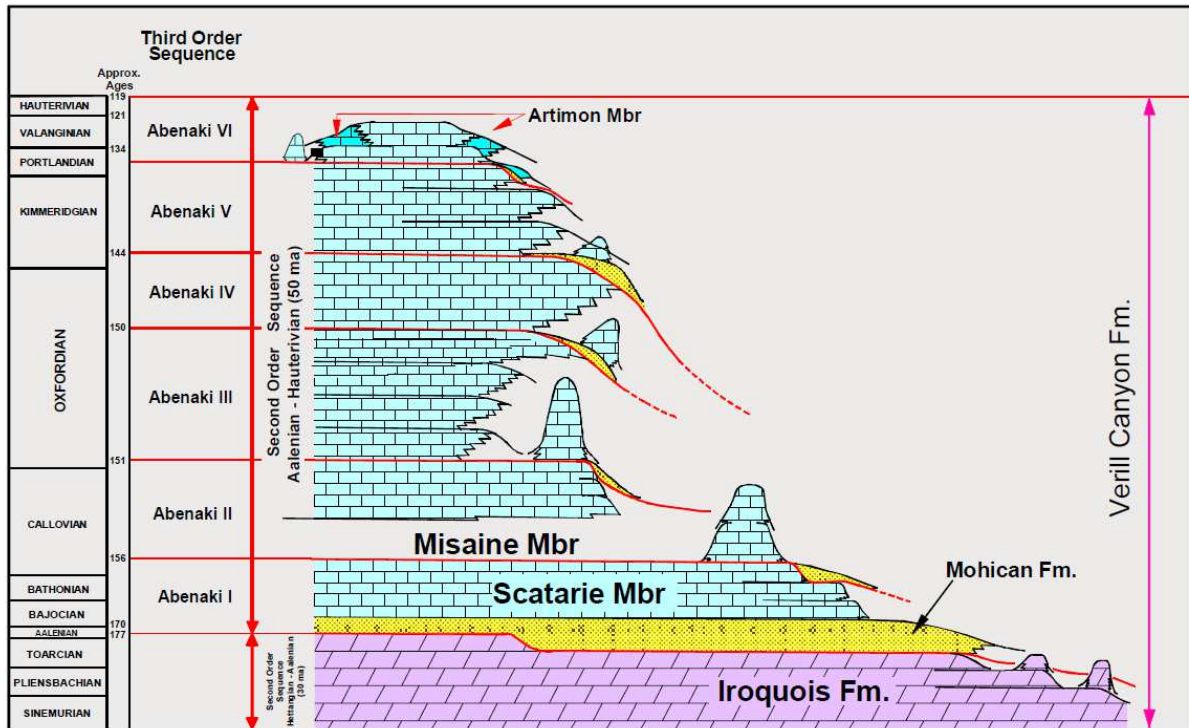


Figure 17: Schematic sequence stratigraphic cross-section, Iroquois through Abenaki Formations (Weissenberger, 2000).

5. Summary and Results

In this study, reflection amplitude and acoustic impedance realisations of the Penobscot 3D seismic survey were methodically interpreted and fully integrated with well data and published regional knowledge of the Sable sub-Basin. There are three key results:

1. Both cubes provide powerful rendition of stratigraphic and small-scale structural features in map-view or horizon-slice view. Lower coastal plain / shallow marine channels in the Logan Canyon section are expressed as subtle, apparently random, amplitude anomalies in cross-section view, but become spatially coherent and obvious on horizon-slices. Similarly, sporadic, subtle dip changes at Top Wyandot Formation form a semi-continuous polygonal network when viewed on horizon-slices.
2. The principle value of the absolute acoustic impedance cube is that it provides direct linkage to lithologies through the acoustic impedance parameter: particularly low impedance sandstones in the Logan Canyon and Missisauga Formations; and in distinguishing high impedance carbonates and low impedance marine shales at the flank of the Abenaki platform. This may have impact for source rock studies.
3. Comparing ‘recursive’, ‘coloured’, ‘constrained sparse spike’ and ‘spectral’ inversions applied at Penobscot we conclude that for our purposes CSSI is the optimum technique for incrementally building large sub-regional scale inversions where we need to balance work-effort, signal-to-noise, careful quantitative mapping of absolute acoustic impedance, and the identification of stratigraphic features on horizon-slices, and we will proceed based on this conclusion. However,

'fast track' inversions may also be suitable for scoping applications and the additional resolution of spectral inversion warrants further investigation. We would be very interested in participating in a comparative study of these inversion results if digital data are available.

6.0 References:

- Ahmad, Q. (2013). Mitigation Exploration Risk of Jurassic Reservoir by Seismic Inversion, Penobscot Area, Sable Sub Basin Nova Scotia, Offshore, Canada. *Journal Geology and Geoscience* 2(3).
- Anselmetti, F. S., & Eberli, G. P. (1993). Controls on sonic velocity in carbonates. *Pure and applied geophysics*, 141(2-4), 288-290.
- Barss, M.S., Bujak, J.P., & Williams, G.L. (1979). Palynological zonation and correlation of sixty-seven wells, eastern Canada. *Geological Survey of Canada*, Paper 78-24.
- Catuneanu, O. (2006). Principles of Sequence Stratigraphy. Amsterdam: Elsevier.
- Canada Nova Scotia Offshore Petroleum Board. Retrieved May 12, 2015, from
<http://www.cnsopb.ns.ca/geoscience/geoscience-overview/exploration-history>
- Cartwright, J. (2014). Are outcrop studies the key to understanding the origins of polygonal fault systems? *Geology*, 42, 559-560.
- Cooke, D., & Cant, J. (2010). Model-based Seismic Inversion: Comparing deterministic and probabilistic approaches. *CSEG Recorder*, 35 (04).

- Deptuck, M.E. & Campbell, D.C. (2012). Widespread erosion and mass failure from the ~51 Ma Montagnais marine bolide impact off southwestern Nova Scotia, Canada. *Canadian Journal of Earth Sciences*, 49(12), 1567-1594.
- Eliuk, L.S. (1978). The Abenaki Formation, Nova Scotia, Canada – A Depositional and Diagenetic Model for a Mesozoic Carbonate Platform. *Bulletin of Canadian Petroleum Geology*, 26(4), 424-514.
- Eliuk, L.S. & Wach, G. (2008). (Ext. abstr. CD, D.E. Brown & N. Watson, eds.) Carbonate and Siliciclastic Sequence Stratigraphy- Examples from the Late Jurassic Abenaki Limestone and West Venture Deltaic Beds, Offshore Nova Scotia, Canada. Central Atlantic Conjugate Margin Conference, Halifax, 410-437.
- Eliuk, L.S. (2010) Regional Setting of the Late Jurassic Deep Panuke Field, Offshore Nova Scotia, Canada – Cuttings Based Sequence Stratigraphy and Depositional Facies Associations - Abenaki Formation Carbonate Margin. *Search and Discovery Article #10259), adapted from oral presentation at AAPG Convention, New Orleans, Louisiana, April 11-14, 2010.*
- Embry, A.F. (2009). Practical Sequence Stratigraphy. *Canadian Society of Petroleum Geologists*, Online at www.cspg.org.
- Given, M. (1977). Mesozoic and Early Cenozoic Geology of Offshore Nova Scotia. *Bulletin of Canadian Petroleum Geology*, 25(1), 63-91.
- Hansen, Møller, D., Shimeld, J.W., Williamson, M. A., & Lykke-Anderse, H. (2004). Development of a major polygonal fault system in Upper Cretaceous chalk and Cenozoic mudrocks of the Sable Subbasin, Canadian Atlantic margin. *Marine and Petroleum Geology* 21, 1205–1219.

- Hantschel, T., & Kauerauf, A.I. (2009). Fundamentals of Basin and Petroleum Systems Modeling. Springer-Verlag Berlin Heidelberg.
- Ings, Steven J. R., MacRae, A., Shimeld, J.W., & Georgia Pe-Piper. (2005). Diagenesis and porosity reduction in the Late Cretaceous Wyandot Formation, Offshore Nova Scotia: a comparison with Norwegian North Sea chalks. *Bulletin of Canadian Petroleum Geology*, 53(3), 237-249.
- Jansa, L.F. & Wade, J.A. (1975). Geology of the continental margin off Nova Scotia and Newfoundland: in Offshore Geology of Eastern Canada, Vol. 2, Regional Geology, Vander Linden, W.J.M. and Wade, J.A. (Eds.), *Geological Survey of Canada*, (74-30), 51-106.
- Jansa, Lubomir F, & Noguera Urrea, V.H. (1990). Geology and Diagenetic History of Overpressured Sandstone Reservoirs, Venture Gas Field, Offshore Nova Scotia, Canada. *The American Association of Petroleum Geologist Bulletin*, 74(10), 1640-1658.
- Kidston, A.G., Brown, D.E., Smith B.M., & Altheim, B. (2005). The Upper Jurassic Abenaki Formation Offshore Nova Scotia: A Seismic and Geologic Perspective. *Canada- Nova Scotia Offshore Petroleum Board*.
- Kumar, N. & Negi, S.S. (2012). Low frequency modeling and its impact of seismic inversion data. 9th Biennial International Conference & Exposition on Petroleum Geophysics.
- Labails, C., Olivet, J., Aslanian, D., & Roest, W. (2010). An alternative early opening scenario for the Central Atlantic Ocean. *Earth and Planetary Science Letters*, 297(3-4), 355-368.
- Lancaster, S., & D. Whitcombe, 2000, Fast track ‘coloured’ inversion: 70th Annual International Meeting, SEG, *Expanded Abstracts*, 1572–1575
- Lines, L.R. & Alam M. (2013). Synthetic seismograms, Synthetic Sonic Logs and Synthetic Core, *CSEG Recorder*, 38(04).

- Lindseth, R.O. (1979). Synthetic sonic logs – a process for stratigraphic interpretation: *Geophysics*, 44, 3-26.
- McIver, N.L. (1972). Mesozoic and Cenozoic stratigraphy of the Nova Scotia Shelf. *Canadian Journal of Earth Sciences*, 9, 54-70.
- Miall, A.D. (ed), (2008). Sedimentary basins of the world. The sedimentary basins of the United States and Canada. Elsevier B.V.
- Miall, A. (2010). The geology of stratigraphic sequences (2nd ed). Berlin: Springer.
- R.M. Mitchum, JR., Vail, P.R & Thompson, S. (1977). Seismic Stratigraphy and Global Changes of Sea Level, Part 2: The Depositional Sequence as a Basic Unit for Stratigraphic Analysis. in Seismic Stratigraphy: Applications to Hydrocarbon Exploration (AAPG Memoir 26) Payton, Charles E.(ed) *American Association of Petroleum Geologists*, Tulsa, Oklahoma USA.
- Mukhopadhyay, P. K., Brown D.E., Kidston A.G., Bowman T.D., Faber J., & Harvey P.J. (2003). Petroleum Systems of Deepwater Scotian Basin, Eastern Canada: Challenges for Finding Oil versus Gas Provinces. Offshore Technology Conference held in Houston, Texas, U.S.A.
- Natural Resources Canada, (2009). Geology of the Scotian Margin. www.nrcan.gc.ca.
- Olsen, P.E., Kent, D.V., Fowell, S.J., Schlische, R.W., Jack, M.O., & LeTourneau, P.M. (2000). Implications of a comparison of the stratigraphy and depositional environments of the Argana (Morocco) and Fundy (Nova Scotia, Canada) Permian-Jurassic basins, in Oujidi, M. and Et-Touhami, M., eds., *Le Permien et le Trias du Maroc, Actes de la Première Réunion du Groupe Marocain du Permien et du Trias: Oujda, Hilal Impression*, 165-183

- Olsen, P.E., Kent, D.V., Et-Touhami, M., & Puffer, J. H. (2003). Cyclo-, magneto-, and biostratigraphic constraints on the duration of the CAMP event and its relationship to the Triassic-Jurassic boundary, in Hames, W.E., McHone, J.G., Renne, P.R, Ruppel, C. (eds.), *The Central Atlantic Magmatic Province: Insights From Fragments of Pangaea, Geophysical Monograph Series, (136)*, 7-32.
- Pendrel, J. (2001). Seismic Inversion – The best tool for reservoir characterisation, *CSEG Recorder*, 26(1).
- Pendrel, J. (2006). The New reservoir Characterisation, *CSEG Recorder*, 31(special ed).
- Pe-Piper, G., & Mackay, M. (2006). Provenance of Lower Cretaceous sandstones onshore and offshore Nova Scotia from electron microscope geochronology and chemical variation of detrital monazite. *Bulletin of Canadian Petroleum Geology*, 54, 366-379.
- Puryear, C.I., and J. P. Castagna, (2008). Layer-thickness determination and stratigraphic interpretation using spectral inversion: Theory and application, *Geophysics*, 73, R37-R48.
- Qayyum, F., Catuneanu, O., & Bouanga, C.E. (2014). Sequence stratigraphy of a mixed siliciclastic-carbonate setting, Scotian Shelf, Canada. *SEG Interpretation Journal*, 3(2), SN21-SN37.
- Richards, F.W., Fairchild, L.H., Vrolijk, P.J, & S.J., Hippler, S.J. (2008). Reservoir connectivity analysis, hydrocarbon distribution, resource potential and production performance in the clastic plays of the Sable Subbasin, Scotian Shelf, in D.E. Brown, ed., Extended Abstracts Volume: Central Atlantic Conjugate Margins Conference, Halifax, p.165-185, ISBN:0-9810595-1.
- Robertson Research International Ltd. (2000). Frontier Reservoirs of the North Atlantic. Canada Nova Scotia Offshore Petroleum Board, 1, 270-271.

- Sangree, J.B., and Widmier, J.M. (1979). Interpretation of depositional facies from seismic data. *Geophysics*, 44, 131-160.
- Sayers, J.E. (2013). Enhancement of the Geological Features of the Scotian Basin by the Application of Spectral Inversion, Offshore Nova Scotia. *MSC Thesis University of Houston*. Retrieved May 12, 2015 from http://repositories.tdl.org/uh-ir/bitstream/handle/10657/458/SAYERS_THESIS_2013.pdf?sequence=1&isAllowed=y.
- Shimeld, J. (2004). A comparison of salt tectonic sub-provinces beneath the Scotian Slope and Laurentian Fan, 24th Annual GCS-SEPM Foundation Bob F. Perkins Research Conference, Houston, 291-306.
- Sibuet, J.C., Rouzo, S., & Shrivastava, S. (2012). Plate tectonic reconstructions and paleogeographic maps of the Central and North Atlantic oceans. *Canadian Journal of Earth Sciences*, (49) 12, 1395-1415.
- Smith, B. M., Deptuck, M. E., & Kendell, K. L. (2010). Upper Cretaceous mass transport systems above the Wyandot Formation chalk, offshore Nova Scotia, In: Submarine Mass Movements and Their Consequences, Advances in Natural and Technological Hazards Research, Edited by: D. Mosher et al., Kluger-Springer Book Series, 28, 605-616.
- Stoker, M.S., Pheasant, J.B., & Josenans, H. (1997). Seismic methods and interpretation. In, T.A. Davies, T. Bell, A.K. Cooper, H. Josenhans, L. Polyak, A. Solheim, M.S. Stoker, J.A. Stravers (Eds.), *Glaciated Continental margins: An atlas of acoustic images*, 9-19.
- Vail, P.R, R.M. Mitchum, JR; S. Thompson. (1977). Seismic stratigraphy and global changes in sea level, Part 3: Relative changes of sea level from coastal onlap. *Seismic Stratigraphy: Applications to Hydrocarbon Exploration*. C.E Payton, *American Association of Petroleum Geologists*, Tulsa. AAPG Memoir 26: 49-62.

- Wade, J.A. & MacLean, B.C. (1990). Chapter 5 - The geology of the southeastern margin of Canada, Part 2: Aspects of the geology of the Scotian Basin from recent seismic and well data. In: M.J. Keen and G.L. Williams (Eds.), *Geology of Canada No.2 - Geology of the continental margin of eastern Canada*. *Geological Survey of Canada*, (2), 190-238.
- Wade, J.A. (1991). *Scotian Shelf – East Coast Basin Series*, Atlantic Geoscience Centre. *Geological Survey of Canada*, 71-73.
- Wade, J.A., & MacLean, B.C. (1993). East coast basin atlas series: seismic markers and stratigraphic picks in Scotian Basin wells. *Atlantic Geoscience Centre, Geological Survey of Canada*, p. 276.
- Wade, J.A., MacLean, B.C., & Williams, G.L. (1995). Mesozoic and Cenozoic stratigraphy, eastern Scotian Shelf: new interpretations. *Canadian Journal of Earth Sciences*, 32, 1462-1473.
- Weissenberger, J.A.W., Harland, N., Hogg, J., & Sylonyk, G., 2000. Sequence stratigraphy of Mesozoic Carbonates, Scotian Shelf, Canada. In: *GeoCanada 2000 – The Millennium Geoscience Summit, Joint Convention of the CSPG, CSEG, GAC, MAC, CGU & CWLS, Conference CD-ROM disk*, 1262.
- Weissenberger, J.A.W., Wierzbicki, R.A., & Harland, N.J. (2006). Carbonate Sequence Stratigraphy and Petroleum Geology of the Jurassic Deep Panuke Field, Offshore Nova Scotia, Canada, in P.M. Harris and L.J. Weber (eds.), *Giant Hydrocarbon reservoirs of the World: From rocks to reservoir characterization and modeling*: AAPG Memoir 88/SEPM Special Publication, p. 395-431.
- Wierzbicki, R., Gillen, K., Ackermann, R., Harland, N., Eliuk, L., & J. Dravis. (2005). Interpretation of a fractured dolomite core: Margaree F- 70, Deep Panuke, Nova Scotia,

Canada, Canadian Society of Petroleum Geologists Annual Core Conference in conjunction with AAPG Annual Convention in Calgary (extended abstract-article in this CSPG CD).

- Wierzbicki, R., Dravis, J.J., Al-Aasm, I., & Harland, N. (2006). Burial dolomitization and dissolution of Upper Jurassic Abenaki platform carbonates, Deep Panuke reservoir, Nova Scotia, Canada. *AAPG Bulletin*, 90(11), 1843-1961.
- Weston, J.F., MacRae, R.A., Ascoli, P., Cooper, M.K.E., Fensome, R.A., Shaw, D., & Williams, G.L. (2012). A revised biostratigraphic and well-log sequence stratigraphic framework for the Scotian Margin, offshore eastern Canada. *Canadian Journal of Earth Sciences*, (49)12, 1417-1462.
- Williams, H., and Grant, A.C. 1998. Tectonic assemblages, Atlantic Region, Canada. 1:3,000,000 map. Geological Survey of Canada, Open File 3657.

7.0 Acknowledgments

We would like to acknowledge and thank Schlumberger, Jason Geophysical (a CGG Company), their donations of software, Canstrat Ltd for their donations of digital lithological logs and Divestco for their donation of digital wireline data and well reports to the Basin and Reservoir lab at Dalhousie University. We would also like to thank the CNSOPB and the GSC for the full suite of well reports, wireline data, core data, velocity data, pressure data, formation tops and lithological logs. We would also like to acknowledge Carlos Wong at Dalhousie University for his endless help and support.

Interpretation of the Penobscot 3D Seismic Volume Using Constrained
Sparse Spike Inversion, Sable sub-Basin, Offshore Nova Scotia: **Highlights**

- We examine the constrained sparse spike inversion technique at Penobscot, NS.
- We examine the effectiveness of CSSI in mapping absolute acoustic impedance.
- Reflection amplitude and acoustic impedance data were interpreted and integrated.
- Acoustic impedance provides direct linkage to lithologies.